Journal of Asian Earth Sciences xxx (2010) xxx–xxx

Contents lists available at ScienceDirect

Journal of Asian Earth Sciences

journal homepage: www.elsevier.com/locate/jseaes

Alkaline series related to Early-Middle Miocene intra-continental rifting in a collision zone: An example from Polatlı, Central Anatolia, Turkey

Abidin Temel [a,*], Tekin Yürür [a], Pınar Alıcı [b], Elif Varol [a], Alain Gourgaud [c], Hervé Bellon [d], Hünkar Demirbağ [b]

[a] Hacettepe University, Dept. of Geological Engineering, 06800, Beytepe-Ankara, Turkey
[b] Maden Tetkik ve Arama Genel Müdürlüğü, Maden Etüt ve Arama Dairesi Başkanlığı, 06520 Balgat, Ankara, Turkey
[c] Université Blaise Pascal, OPGC, Laboratoire CNRS "Magmas et Volcans" 5 rue Kessler-63038, Clermont-Ferrand Cedex, France
[d] IUEM, UMR 6538 "Domaines océaniques", Université de Bretagne Occidentale 6, Avenue Le Gorgeu, BP 809, 29285 Brest cedex, France

ARTICLE INFO

Article history:
Received 18 March 2009
Received in revised form 16 December 2009
Accepted 31 December 2009
Available online xxxx

Keywords:
Basaltic lavas
Mantle modification
Neo-Tethys Ocean
Polatlı
Central Anatolia
Turkey

ABSTRACT

A large volcanic area (~7600 km^2), the Galatean Volcanic Province (GVP), developed in northwest Central Anatolia during the Miocene along the Neo-Tethys Ocean suture zone possibly by post-collisional processes. The GVP mainly comprises 20–14 My old acid to intermediate volcanites with a geochemical signature indicating a mantle source modified by earlier (Late Cretaceous) subduction-related events. 100 km south of the GVP, near Polatlı, Ankara, basaltic rocks that cover large areas are intercalated with the Miocene deposits of the Beypazarı basin, an intra-continental subsidence zone at the southwest of the GVP. Field observations, geochemistry and K–Ar age dating of the Polatlı volcanites show that they are Early (19.9 Ma) to mid (14.1 Ma) Miocene in age, covering an area as large as 215 km^2. Variations in lava thickness and the thickness of the underlying silicified/baked zones suggest that the basaltic lavas erupted from a southern source, possibly from the Eskişehir fault zone, and flowed northwards. Most Polatlı samples have chemical compositions that indicate derivation from a mantle source with crustal contamination during ascent. They do not display any characteristic to suggest a subductional component. Although the GVP and Polatlı lavas formed close in time and space, they were derived from different mantle sources. Considering the positions of these two magmatic regions with regard to the Tethyan suture zone, we propose that the mantle beneath the GVP and near the suture zone memorised the earlier subduction while the mantle beneath Polatlı that is located about 100 km further from the suture zone remained apparently unchanged. After a significant volume of magma was consumed in the GVP, a later (~10 My) and last activity (Güvem activity) has produced quantitatively much less basaltic rocks where this subductional signature seems to completely disappear. Considering that the western Anatolian crust is proposed to undergo extension since the Late Oligocene–Early Miocene times, the Early Miocene intraplate Polatlı activity may have developed within this extensional tectonic regime. Combined with regional data, Polatlı data also provide broad estimations on how long a subductional event continues to modify the mantle after the subduction ceased (at least ~20 My), how long the subductional signature is preserved during significant magmatism (between 6 and 10 My) and how far the subductional effect disappears laterally on the mantle with respect to the collision zone (<100 km).

1. Introduction

In Anatolia, the latest major tectonic events began with the collision between the Eurasian, African and Arabian plates during Middle-Late Miocene times (Şengör and Kidd, 1979; Şengör, 1980; Şengör et al., 1985). The collision resulted in the lateral extrusion of the Anatolian lithospheric block, escaping from the convergence zone in the east, towards the west where it overrides the subducting African oceanic plate. Widespread volcanism has accompanied this period and numerous workers have produced data from Anatolian volcanic districts to discuss the origin, age, and tectonic settings of the volcanic rocks erupted during this period (Innocenti et al., 1982; Tokel, 1984; Tokel et al., 1988; Gülen, 1990; Pearce et al., 1990; Savascın, 1990; Savascın and Güleç, 1990; Yılmaz, 1990; Güleç, 1991; Keller et al., 1992; Notsu et al., 1995; Wilson et al., 1997; Alıcı et al., 1998, 2001; Buket and Temel, 1998; Tankut et al., 1998; Temel et al., 1998a,b; Temel, 2001; Varol et al., 2007). In this study, we report new data on field observations, geochemistry and K–Ar ages of basaltic rocks from Central Anatolia, particularly those outcropping near the Galatean Volcanic Province (GVP) (Fig. 1). The GVP corresponds to the Miocene part of a Tertiary magmatic belt developed at the boundary of the Anatolian block as a result of the subduction of the Neo-Tethys Ocean

* Corresponding author. Fax: +90 312 299 20 34.
E-mail address: atemel@hacettepe.edu.tr (A. Temel).

1367-9120/$ - see front matter © 2010 Elsevier Ltd. All rights reserved.
doi:10.1016/j.jseaes.2009.12.017

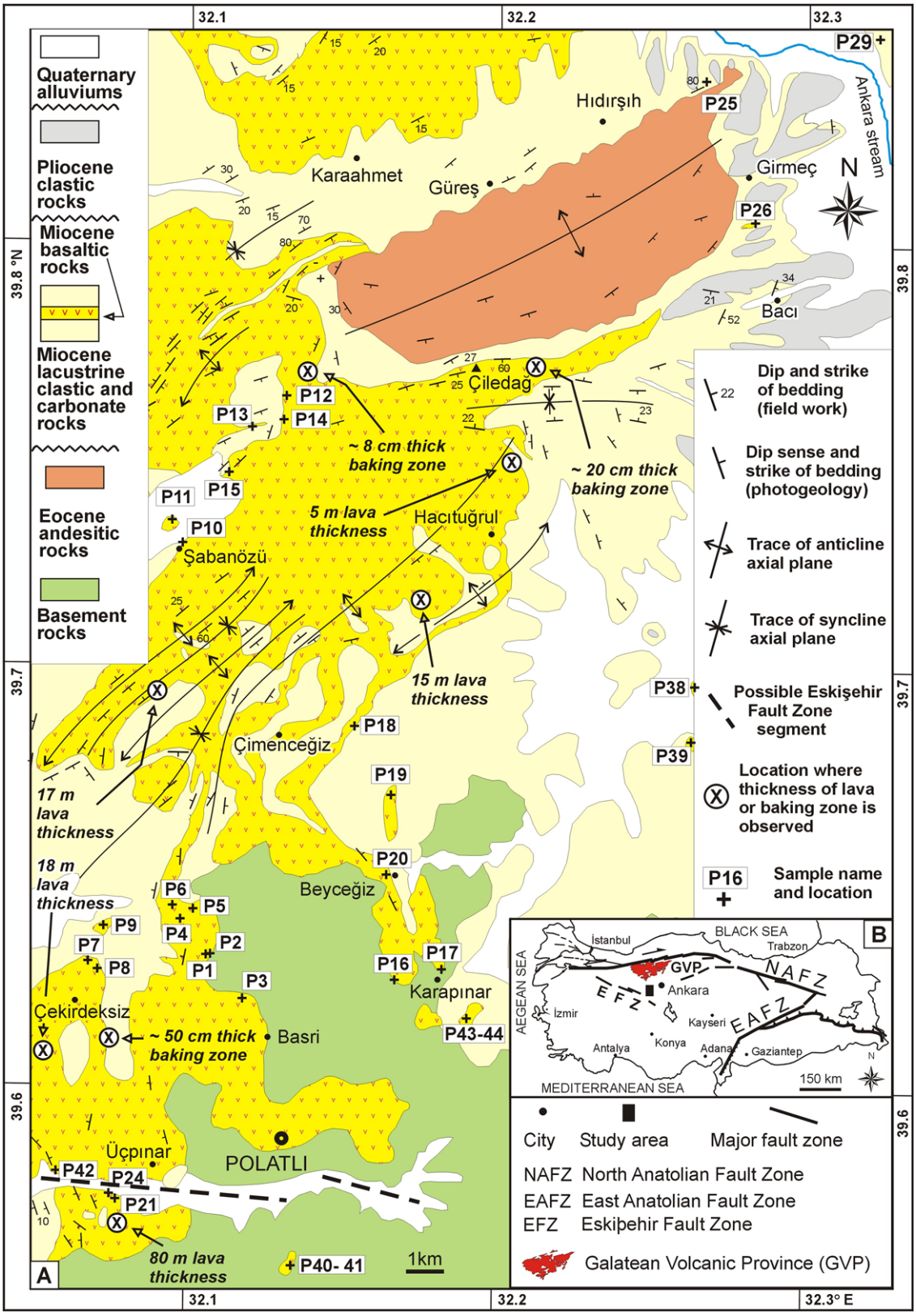

Fig. 1. Generalized geological sketch map of Polatlı (SW Ankara) region (modified from Erol, 1955). Insert map shows the main Anatolian Neogene volcanic rock outcrops and the position of the study area in Turkey.

(Koçyiğit et al., 1995, 2003). Most of the GVP units are of Early Miocene age (Keller et al., 1992; Toprak and Türkecan, 1998; Varol et al., 2008) with acid to intermediate composition volcanic rocks derived from mantle sources modified by subductional processes (Wilson et al., 1997). The GVP rocks are occasionally intercalated with the Miocene intra-continental sediments of the Beypazarı ba-

Please cite this article in press as: Temel, A., et al. Alkaline series related to Early-Middle Miocene intra-continental rifting in a collision zone: An example from Polatlı, Central Anatolia, Turkey. Journal of Asian Earth Sciences (2010), doi:10.1016/j.jseaes.2009.12.017

sin that surrounds the GVP to the west (İnci, 1991). About 100 km south of this province, near the Polatlı town at the west of Ankara, the Miocene deposits are alternated with basaltic rocks of poorly known geochemical characteristics (Yurtyeri, 1989) and radiometric ages. In this paper, we report new data on field, geochemical and radiometric age characteristics of these basaltic rocks. Using this information, we discuss the origin, age, spreading center location and tectonic environment in which these rocks erupted. The geochemistry of these volcanic rocks suggests a magma source different from those of the northern GVP volcanites. Comparing these two magmatic domains similar in time and space, we also discuss the geotectonic environments in which they have formed and evolved.

2. Geological setting

Geological features of the study area are shown in Fig. 1. The area comprises Mesozoic-Tertiary basement rocks and Miocene volcano-sedimentary rocks of the Beypazarı basin and the Galatean Volcanic Province (GVP).

The basement is composed of sedimentary rocks deposited during the Jurassic-Cretaceous and Eocene times (Ünalan et al., 1976; Hakyemez et al., 1986). Volcanic material is found within Eocene sediments. The Eocene age of the earlier volcanic activity is confirmed by previous studies (e.g. Seyitoğlu and Büyükönal, 1995). Our radiometric age determinations indicate that the ages of the Polatlı alkaline basaltic rocks are in 14–20 Ma (Table 1). There are, however, older volcano-sedimentary units within the GVP (Campanian volcanites reported by Koçyiğit et al. (2003)).

The Lower–Middle Miocene Beypazarı basin deposits are detritic and carbonate rocks with coal-bearing siltstones that represent alluvial fan, river and lacustrine sediments (Siyako, 1984; İnci et al., 1988). The Late Miocene (?) is represented by lake deposits including gypsum, gypsiferous marl, tuffite, pebblestone, sandstone and mudstones (Hakyemez et al., 1986; İnci, 1991).

The Polatlı basaltic lavas are found intercalated with the Early–Middle Miocene deposits of the Beypazarı basin. The maximum thickness the basaltic lavas reach is about 80 m (Yurtyeri, 1989), at the south of the study area (Fig. 1) whereas the sedimentary column has a maximum thickness of ~170 m (our field data). Based on geologic maps and field observations, we estimate the lavas to cover a surface of about 215 km^2 with a volume less than 2 km^3. Rocks samples for geochemical analyses and age determinations are collected from their outcrops near Üçpınar (Fig. 1).

3. Analytical techniques

K–Ar dating was performed on whole-rock samples at Brest University, France. After crushing and sieving, the rock fraction of 0.30–0.15 mm size was cleaned with distilled water and retained for analytical purposes: (i) one aliquot was powdered for K analysis by atomic absorption after HF chemical attack, and (ii) 0.5–0.15 mm grains were used for argon isotopic analysis. Argon was extracted under high vacuum by induction heating of a molybdenum crucible containing the sample grains. Gases were cleaned on two titanium sponge furnaces and finally purified by using two Al–Zr SAES getters. The isotopic dilution method was applied using a ^{38}Ar spike buried as ions in aluminium targets along the original procedure described by Bellon et al. (1981). Isotopic composition of argon and concentration of radiogenic ^{40}Ar were determined using a 180°-geometry stainless steel mass spectrometer with a 642 Keithley amplifier.

Ages are listed with their respective characteristic parameters in Table 1 and are calculated using the constants recommended by Steiger and Jäger (1977) and errors at ±1 sigma level are calculated following the equation of Mahood and Drake (1982).

Mineral compositions of the Polatlı samples were determined using an automatic wavelength-dispersive Cameca-SX 100 electron microprobe at Blaise Pascal University, Department of Geology, Clermont-Ferrand, France. Counting times for individual elements and sample currents were 10 s and 10–12 nA, respectively. The chemical analyses of minerals are available from the corresponding author on request.

Whole-rock major-element compositions were determined on fused discs, and trace elements on pressed powder pellets, using a PW1480 Philips XRF spectrometer in the Department of Geological Engineering, Hacettepe University of Ankara, Turkey. Sample preparation for major and trace elements have been described in Alıcı et al. (1998).

Trace and rare earth element analyses of whole-rock samples were determined by solution ICP-MS at the Universite Blaise Pascal University, Clermont-Ferrand, France on a VG elemental PQ2 instrument. The analytical technique largely followed by Ionov et al. (1992) and Ionov and Harmer (2002). 100 mg of whole-rock powdered samples were dissolved in HF–HNO_3–$HClO_4$ mixture, evaporated to incipient dryness, then evaporated twice at about 140 °C with 0.25 ml of $HClO_4$ to destroy insoluble fluorides. The dry sample was taken up for analysis in 2% HNO_3 with a small amount of HCl. Attempts to use pure 2% HNO_3 for sample take-up failed because of formation of dark precipitates from an initially clear solution, but the addition of several drops of HCl produced clear, stable solutions, possibly due to cation complexing with Cl^-. Composite synthetic pure element solutions were used as external standards In an Bi were added to both sample and external standard solutions as internal standards. BHVO-1 reference sample was analysed as an unknown for quality control.

For isotopic analyses, sample powders (~150 mg) were washed in cold 2 N HCl for 24 h prior to dissolution in HF. Sr and Nd were sequentially separated using standard ion-exchange techniques at Blaise Pascal University, Clermont-Ferrand, France. Mass-spectrometric analyses were done at the same university using a VG 54E mass spectrometer in the double collection mode. Sr-isotopic ratios were normalized to $^{86}Sr/^{88}Sr$: 0.1194 and Nd-isotopic ratios were normalized to $^{146}Nd/^{144}Nd$: 0.7219.

4. Mineralogy

The Polatlı basaltic rocks are porphyritic, with variable amounts of plagioclase, clinopyroxene, olivine and oxide phenocrysts (Fig. 2). The groundmass shows microlitic texture and is composed of plagioclase, clinopyroxene and olivine microlites.

A summary of the representative composition of minerals from Polatlı lavas presented in Table 2.

Table 1
K/Ar age results of Polatlı volcanic rocks.

Sample no.	Age (My)	K_2O (wt.%)	Weight (g)	$^{40}Ar^*/g$ (10^{-7} cm^3)	$^{40}Ar^*$ (%)	^{36}Ar exp (10^{-9} cm^3)	Analysis number
P-24	19.9 ± 1.0	1.49	0.4159	9.59	22.2	4.74	5410
P-41	14.1 ± 0.3	2.35	0.5099	10.74	59.0	1.29	5413

Please cite this article in press as: Temel, A., et al. Alkaline series related to Early-Middle Miocene intra-continental rifting in a collision zone: An example from Polatlı, Central Anatolia, Turkey. Journal of Asian Earth Sciences (2010), doi:10.1016/j.jseaes.2009.12.017

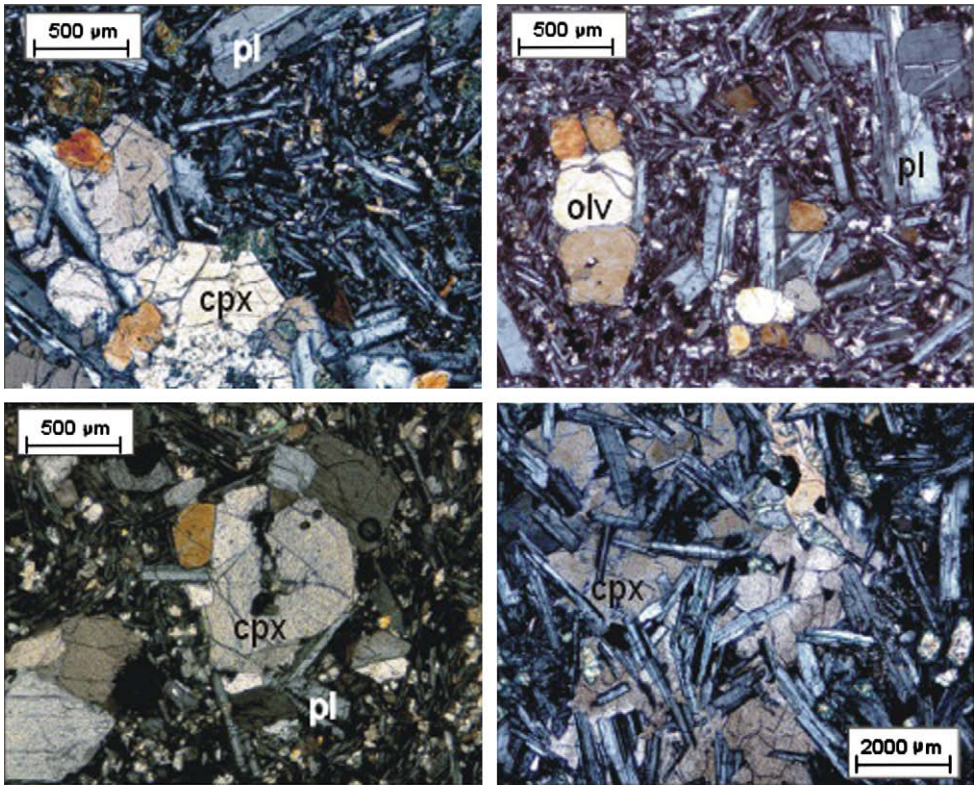

Fig. 2. Microphotographs of representative samples from Polatlı volcanic rocks (olv: olivine; cpx: clinopyroxene; pl: plagioclase).

Table 2
General mineral composition for the selected samples from Polatlı volcanic rocks.

	Phenocrysts	Microlites
Plagioclase		
An	35–73	33–69
Clinopyroxene		
Wo	41–50	46–48
En	35–50	38–43
Fs	8–17	10–15
Olivine		
Fo	59–88	
Ti-Manyetit		
wt.%		
FeO(*t*)	63–71	
TiO_2	23–28	

Abbreviations: An: anorthite; Wo: wollastonite; En: enstatite; Fs: ferrosillite; Fo: forsterite.

Plagioclase occurs as clear euhedral phenocrysts and microlites which are generally zoned and twinned. Plagioclase composition of phenocrysts and microlites range from andesine An_{35} to bytownite An_{73} and andesine An_{33} to labradorite An_{69}, respectively (Table 3). Some of the plagioclase phenocrysts exhibit patterns of reverse zoning with calcic rims and more sodic cores.

Clinopyroxenes are Mg-rich (En35–50) and are represented by diopside and augite, according to nomenclature proposed by Morimoto (1988). Most of the phenocrysts are reversely zoned (Fe-depletion and Ca, Mg-enrichment toward their rims) (Table 4).

Olivine is well represented by rounded grains. The Fo composition of olivine crystals ranges from Fo_{59} to Fo_{88} (Table 5). Most of the olivine phenocrysts are normally zoned (Mg depletion toward their rims). Reversely zoned olivine phenocrysts are also observed.

Oxides occur as subhedral crystals and they are titanomagnetite in composition (Table 6).

Zoning are common for plagioclase and clinopyroxene phenocrysts, and suggesting that these may not be in equilibrium with the melt.

5. Geochemistry

5.1. Major-oxide geochemistry

Major-oxides, trace, and rare earth element and Sr–Nd isotopic compositions of representative samples from Polatlı region are listed in Tables 7. All major-oxides have been normalized to 100% on an anhydrous basis. Data are plotted on the total alkali vs. silica diagram (Le Bas et al., 1986) with subalkaline-alkaline dividing line of Miyashiro (1978) for the purpose of classification (Fig. 3). According to these diagrams, all the samples exhibit an alkaline trend. They range in composition from basalt, trachybasalt to basaltic trachyandesite.

Plots of SiO_2 vs. selected major-oxides are shown in Fig. 3. Increasing SiO_2 is correlated with decreasing of MgO, CaO, TiO_2 and increasing K_2O. These variations may correspond to those expected from fractional crystallization process, even though plots are scattered. For instance, MgO, CaO and TiO_2 decrease regularly with increasing silica contents, which is qualitatively consistent with the predominance of olivine, clinopyroxene, Ca-plagioclase and Fe–Ti oxides fractionation. K_2O exhibit slightly positive correlations with SiO_2 (Fig. 4) which may indicate a fractionation trend. The overall trends in Harker diagram are generally scattered. This may result from partial melting and/or crustal contamination in addition to fractional crystallization processes. Thus, in the next sections, we will examine the effects of those processes in the genesis and evolution of Polatlı lavas.

As a consequence, with regard to the correlations of SiO_2 with major-oxides, fractional crystallization processes is effective in the evolution of Polatlı lavas, but the scattering of plots can be related to partial melting and/or crustal contamination.

Please cite this article in press as: Temel, A., et al. Alkaline series related to Early-Middle Miocene intra-continental rifting in a collision zone: An example from Polatlı, Central Anatolia, Turkey. Journal of Asian Earth Sciences (2010), doi:10.1016/j.jseaes.2009.12.017

Table 3
Selected microprobe analyses of feldspar. Number of cations on the basis of 8 oxygen.

	Plagioclase											
	P-1						P-7					
	c→	*b*	*c*→	*k*	mic	mic	*c*→	*b*	mic	*c*→	*b*	mic
SiO_2	52.57	49.63	50.21	50.48	52.73	51.12	52.51	51.26	53.98	52.85	49.74	49.70
Al_2O_3	29.22	31.02	30.76	30.18	29.32	29.89	29.38	30.78	28.65	29.29	31.06	30.94
FeOt	0.37	0.62	0.63	0.61	0.70	0.80	0.35	0.49	0.46	0.26	0.66	0.70
MgO	0.01	0.03	0.08	0.11	0.02	0.12	0.06	0.02	0.01	0.05	0.02	0.04
CaO	11.75	14.03	14.00	13.75	11.86	13.08	12.47	13.67	11.20	12.19	14.54	13.95
Na_2O	4.45	3.19	3.48	3.67	4.68	3.85	4.29	3.57	5.06	4.63	3.27	3.30
K_2O	0.40	0.43	0.25	0.25	0.42	0.28	0.30	0.32	0.34	0.23	0.23	0.29
Total	98.77	98.95	99.39	99.05	99.72	99.13	99.35	100.11	99.70	99.49	99.52	98.92
Si	2.410	2.287	2.300	2.318	2.392	2.345	2.396	2.332	2.445	2.403	2.279	2.290
Al	1.579	1.685	1.661	1.633	1.568	1.616	1.580	1.650	1.530	1.570	1.677	1.680
Fe^{3+}	0.014	0.024	0.024	0.023	0.026	0.030	0.013	0.019	0.017	0.010	0.025	0.027
Fe^{2+}	0.000	0.000	0.000	0.000	0.000	0.000	0.000	0.000	0.000	0.000	0.000	0.000
Mg	0.001	0.002	0.005	0.008	0.001	0.008	0.004	0.001	0.001	0.003	0.002	0.003
Ca	0.577	0.692	0.687	0.676	0.576	0.643	0.610	0.666	0.544	0.594	0.714	0.689
Na	0.396	0.285	0.309	0.327	0.412	0.342	0.379	0.314	0.444	0.408	0.290	0.295
K	0.024	0.025	0.014	0.015	0.024	0.016	0.017	0.019	0.020	0.013	0.013	0.017
Ab	39.72	28.44	30.59	32.12	40.71	34.17	37.67	31.43	44.05	40.20	28.52	29.47
An	57.87	69.06	68.02	66.40	56.92	64.24	60.64	66.67	53.97	58.52	70.21	68.83
Or	2.41	2.50	1.39	1.47	2.37	1.60	1.69	1.90	1.98	1.28	1.28	1.70

	P-15									P-19			
	c	*c*→	*b*	*c*→	*k*	*c*→	*b*	mic	mic	*c*→	*b*	mic	*c*→
SiO_2	47.79	49.67	52.17	49.50	48.98	48.71	50.06	49.54	59.24	59.05	54.57	56.07	54.48
Al_2O_3	31.32	30.91	29.59	31.79	31.80	30.98	30.49	30.79	24.93	25.29	28.71	26.89	28.39
FeOt	0.58	0.59	0.63	0.48	0.63	0.61	0.79	0.64	0.31	0.32	0.29	0.66	0.39
MgO	0.04	0.12	0.00	0.10	0.06	0.05	0.07	0.05	0.02	0.04	0.07	0.05	0.08
CaO	15.28	14.64	13.11	14.39	14.77	13.65	13.61	14.17	6.91	7.55	11.09	9.47	10.48
Na_2O	2.93	3.03	4.19	2.91	2.90	3.13	3.60	3.35	7.19	6.55	4.98	5.96	5.34
K_2O	0.31	0.12	0.13	0.37	0.43	0.23	0.32	0.30	0.69	1.93	0.45	0.71	0.70
Total	98.25	99.09	99.83	99.52	99.56	97.35	98.93	98.84	99.29	100.73	100.16	99.81	99.84
Si	2.219	2.289	2.373	2.270	2.245	2.281	2.302	2.283	2.665	2.626	2.461	2.526	2.457
Al	1.713	1.679	1.586	1.718	1.718	1.709	1.652	1.672	1.322	1.326	1.526	1.428	1.509
Fe^{3+}	0.023	0.022	0.024	0.018	0.024	0.024	0.030	0.025	0.012	0.012	0.010	0.025	0.015
Fe^{2+}	0.000	0.001	0.000	0.000	0.000	0.000	0.000	0.000	0.000	0.000	0.001	0.000	0.000
Mg	0.003	0.008	0.000	0.006	0.004	0.003	0.005	0.003	0.001	0.003	0.005	0.004	0.005
Ca	0.760	0.723	0.639	0.707	0.726	0.685	0.670	0.699	0.333	0.360	0.536	0.457	0.506
Na	0.264	0.271	0.370	0.259	0.257	0.284	0.321	0.299	0.628	0.565	0.435	0.520	0.467
K	0.018	0.007	0.008	0.022	0.025	0.014	0.018	0.018	0.040	0.109	0.026	0.041	0.040
Ab	25.34	27.07	36.38	26.21	25.50	28.89	31.81	29.43	62.74	54.64	43.63	51.08	46.10
An	72.94	72.23	62.83	71.56	72.02	69.68	66.40	68.80	33.27	34.82	53.76	44.89	49.95
Or	1.73	0.70	0.79	2.23	2.48	1.42	1.78	1.77	4.00	10.54	2.61	4.03	3.95

	P-19								P-24			
	b	mic	*c*→	*b*	*c*→	*b*	*c*→	*b*	c→	b	c→	b
SiO_2	52.18	52.47	52.42	53.41	56.06	53.56	54.62	54.42	52.58	51.93	52.45	52.30
Al_2O_3	30.38	29.40	29.58	28.91	28.02	29.54	28.71	28.10	30.02	30.03	29.16	29.42
FeOt	0.50	0.42	0.26	0.50	0.24	0.48	0.33	0.45	0.23	0.53	0.39	0.46
MgO	0.03	0.13	0.07	0.05	0.08	0.09	0.08	0.10	0.08	0.08	0.06	0.09
CaO	12.79	12.24	12.63	11.71	10.68	12.19	11.64	11.15	13.12	13.55	12.13	12.71
Na_2O	4.14	4.37	4.19	4.59	5.63	4.57	5.23	5.39	4.30	3.91	4.58	4.46
K_2O	0.52	0.65	0.29	0.33	0.51	0.36	0.26	0.46	0.28	0.26	0.35	0.30
Total	100.53	99.68	99.44	99.51	101.21	100.78	100.87	100.07	100.60	100.28	99.13	99.74
Si	2.354	2.383	2.390	2.431	2.493	2.404	2.442	2.447	2.367	2.353	2.391	2.372
Al	1.615	1.574	1.590	1.551	1.469	1.563	1.513	1.490	1.593	1.604	1.567	1.572
Fe^{3+}	0.019	0.016	0.010	0.013	0.009	0.018	0.012	0.017	0.009	0.020	0.015	0.017
Fe^{2+}	0.000	0.000	0.000	0.006	0.000	0.000	0.000	0.000	0.000	0.000	0.000	0.000
Mg	0.002	0.009	0.004	0.003	0.005	0.006	0.006	0.006	0.005	0.005	0.004	0.006
Ca	0.618	0.596	0.617	0.571	0.509	0.586	0.557	0.537	0.633	0.658	0.593	0.618
Na	0.362	0.385	0.371	0.405	0.485	0.398	0.453	0.470	0.375	0.343	0.405	0.392
K	0.030	0.037	0.017	0.019	0.029	0.020	0.015	0.026	0.016	0.015	0.021	0.018
Ab	35.84	37.82	36.92	40.70	47.41	39.64	44.20	45.50	36.62	33.76	39.74	38.13
An	61.19	58.55	61.39	57.39	49.76	58.37	54.34	51.98	61.82	64.76	58.19	60.12
Or	2.97	3.63	1.69	1.91	2.83	1.99	1.46	2.52	1.56	1.48	2.06	1.75

(*continued on next page*)

Please cite this article in press as: Temel, A., et al. Alkaline series related to Early-Middle Miocene intra-continental rifting in a collision zone: An example from Polatlı, Central Anatolia, Turkey. Journal of Asian Earth Sciences (2010), doi:10.1016/j.jseaes.2009.12.017

Table 3 (*continued*)

	P-38					P-41					
	mic	c→	b	c→	b	c→	k	mic	mic	c→	b
SiO_2	50.89	51.39	50.40	50.82	50.49	53.05	53.57	52.83	53.31	52.70	53.17
Al_2O_3	29.98	29.04	29.52	29.45	29.73	29.60	28.70	29.16	29.01	28.99	28.89
FeOt	0.67	0.55	0.57	0.49	0.49	0.52	0.29	0.57	0.48	0.41	0.53
MgO	0.03	0.11	0.07	0.08	0.07	0.01	0.05	0.02	0.02	0.03	0.04
CaO	13.49	12.95	13.21	13.13	13.59	12.01	11.23	12.11	11.64	12.05	11.65
Na_2O	3.96	4.25	3.90	3.83	3.79	4.49	4.75	4.43	4.66	4.60	4.72
K_2O	0.20	0.23	0.23	0.22	0.23	0.21	0.33	0.27	0.29	0.23	0.27
Total	99.21	98.52	97.91	98.01	98.39	99.89	98.90	99.39	99.41	99.01	99.25
Si	2.327	2.363	2.335	2.355	2.330	2.405	2.448	2.407	2.426	2.407	2.422
Al	1.616	1.574	1.612	1.608	1.618	1.581	1.546	1.566	1.556	1.561	1.551
Fe^{3+}	0.026	0.021	0.022	0.019	0.019	0.006	0.000	0.016	0.016	0.016	0.020
Fe^{2+}	0.000	0.000	0.000	0.000	0.000	0.014	0.011	0.006	0.002	0.000	0.000
Mg	0.002	0.008	0.005	0.005	0.005	0.001	0.003	0.002	0.001	0.002	0.002
Ca	0.661	0.638	0.656	0.652	0.672	0.583	0.550	0.591	0.568	0.590	0.569
Na	0.351	0.379	0.350	0.344	0.339	0.395	0.421	0.391	0.412	0.407	0.417
K	0.012	0.014	0.014	0.013	0.014	0.012	0.019	0.016	0.017	0.013	0.015
Ab	34.28	36.76	34.31	34.09	33.07	39.90	42.53	39.18	41.32	40.30	41.66
An	64.55	61.88	64.31	64.62	65.56	58.89	55.56	59.22	56.97	58.42	56.84
Or	1.17	1.36	1.37	1.29	1.37	1.21	1.92	1.60	1.71	1.29	1.50

	P-42						P-43			
	mic	c→	b	mic	c→	b	c→	b	c→	b
SiO_2	50.52	53.34	47.07	57.77	50.28	50.21	51.20	55.33	52.00	51.27
Al_2O_3	30.06	29.70	25.27	26.30	30.04	31.17	30.51	28.41	29.73	29.94
FeOt	0.59	0.59	5.46	0.55	0.73	0.52	0.55	0.65	0.59	0.67
MgO	0.02	0.01	5.70	0.17	0.03	0.00	0.09	0.05	0.09	0.07
CaO	13.94	12.36	10.20	8.35	14.15	14.58	13.97	10.85	13.26	13.62
Na_2O	3.80	4.70	2.50	6.36	3.96	3.43	3.51	5.19	4.05	3.76
K_2O	0.17	0.22	0.20	0.52	0.17	0.18	0.27	0.48	0.32	0.27
Total	99.10	100.91	96.40	100.03	99.35	100.08	100.10	100.96	100.04	99.59
Si	2.317	2.391	2.219	2.591	2.296	2.283	2.329	2.474	2.359	2.341
Al	1.624	1.569	1.404	1.390	1.617	1.671	1.636	1.497	1.590	1.612
Fe^{3+}	0.023	0.022	0.215	0.006	0.028	0.020	0.021	0.022	0.023	0.025
Fe^{2+}	0.000	0.000	0.000	0.015	0.000	0.000	0.000	0.002	0.000	0.000
Mg	0.001	0.001	0.400	0.011	0.002	0.000	0.006	0.003	0.006	0.005
Ca	0.685	0.593	0.515	0.401	0.692	0.710	0.681	0.520	0.645	0.666
Na	0.338	0.409	0.228	0.553	0.350	0.302	0.309	0.450	0.356	0.333
K	0.010	0.012	0.012	0.030	0.010	0.010	0.016	0.027	0.018	0.015
Ab	32.72	40.34	30.20	56.20	33.27	29.55	30.72	45.14	34.94	32.84
An	66.31	58.48	68.21	40.75	65.78	69.47	67.69	52.16	63.30	65.68
Or	0.97	1.18	1.59	3.05	0.95	0.98	1.59	2.71	1.77	1.48

Abrevations: mic: microlite; c: center; b: border; An; anorthite; Ab: albite; Ao: ortoclase.

5.2. Trace and rare earth element geochemistry

Trace element data are listed in Table 7. Ni and Cr contents are generally smaller than the values commonly assumed for primary magmas (Ni = 300–400 ppm; Cr = 300–500 ppm; Jung and Masberg, 1998), presumably reflecting the fractionation of olivine and clinopyroxene.

Harker variation diagrams of trace elements are plotted vs. SiO_2 (Fig. 4). As a whole, plots are scattered. The best correlation is exemplified by Ba and Ni. Concentration of Ni decreases almost regularly with decreasing SiO_2, possibly indicating the fractionation of olivine whereas, Ba correlate positively with SiO_2. These trends may be related to the fractional crystallization processes (Fig. 4). Furthermore, the scattering in the diagrams may also due to partial melting and/or crustal contamination. These processes will be examined in the next sections.

MORB-normalized (Pearce, 1983) trace element abundance patterns of Polatlı lavas are typical of within-plate volcanic rocks (Fig. 5). Incompatible elements are enriched relative to the MORB, except Y and Yb. Most of the Polatlı lavas are enriched in K, Ba and Th and slightly depleted in Ta and Nb (Fig. 5). We consider an asthenospheric mantle source with minor subduction component and/or crustal contamination in the genesis of Polatlı lavas. Furthermore, the depletion in Y, Yb and HREE (Figs. 5 and 6) in Polatlı lavas may indicate a residual garnet signature during partial melting.

Typical features including enrichment in Ba and Th, slight depletion in Nb and Ta are the most significant geochemical characteristics of subduction-related magmas (Fitton et al., 1988; Saunders et al., 1988). Likewise, Nb and Ta are highly sensitive to crustal contamination. Mantle-derived magmas which have been contaminated by continental crust during their ascent to the surface exhibit Nb and Ta negative anomalies (Thompson et al., 1983; Wilson, 1989) in spidergrams. Furthermore, the Ba/Ta and Ba/Nb ratios can be used to separate the basaltic lavas from subduction-related environments from within-plate sources (Gill, 1981; Fitton et al., 1988). High Ba/Ta (>450) and Ba/Nb (>28) ratios are the most striking features of subduction-related magmas (Gill, 1981; Fitton et al., 1988). Ba/Nb and Ba/Ta ratios of the Polatlı lavas range from 7–23 and 123–368, respectively. According to this criterion, crustal contamination processes was responsible for the depletion in Nb and Ta rather than subduction processes.

The rare earth elements data are reported in Table 7. Chondrite-normalized (Nakamura, 1974) REE patterns of the Polatlı lavas have been plotted in Fig. 6. Rare earth element patterns exhibit slightly light REE (LREE) enrichment relative to heavy REE (HREE)

Please cite this article in press as: Temel, A., et al. Alkaline series related to Early-Middle Miocene intra-continental rifting in a collision zone: An example from Polatlı, Central Anatolia, Turkey. Journal of Asian Earth Sciences (2010), doi:10.1016/j.jseaes.2009.12.017

Table 4
Selected microprobe analyses of clinopyroxene. Number of cations on the basis of 6 oxygen.

	Clinopyroxene										
	P-1						P-7				
	c→	*b*	mic	mic	*c*→	*b*	*c*→	*b*	*c*	*c*	*c*
SiO_2	47.26	48.96	49.66	47.22	46.63	50.28	45.17	44.90	46.73	45.20	48.84
TiO_2	2.52	2.34	1.74	3.08	3.01	1.82	3.52	4.37	3.50	4.25	2.48
Al_2O_3	5.45	4.20	3.44	5.03	6.14	3.34	6.38	6.98	5.93	6.56	3.33
FeO	8.37	8.32	7.85	8.57	8.75	7.80	8.84	9.08	8.93	8.80	8.46
MnO	0.18	0.20	0.18	0.23	0.15	0.18	0.15	0.15	0.13	0.16	0.18
MgO	13.15	13.11	14.38	12.62	12.70	14.02	11.75	11.54	12.18	11.50	13.56
CaO	22.58	21.95	22.11	22.01	22.18	22.14	21.73	21.53	21.89	22.28	22.18
K_2O	0.00	0.01	0.11	0.08	0.04	0.00	0.06	0.01	0.00	0.09	0.01
Na_2O	0.52	0.78	0.56	0.69	0.58	0.57	0.62	0.69	0.70	0.75	0.58
Total	100.01	99.86	100.02	99.54	100.18	100.15	98.22	99.24	99.98	99.60	99.62
Si	1.758	1.824	1.837	1.771	1.736	1.863	1.720	1.698	1.749	1.702	1.827
Ti	0.070	0.065	0.048	0.087	0.084	0.051	0.101	0.124	0.098	0.120	0.070
Al	0.239	0.185	0.150	0.222	0.270	0.146	0.286	0.311	0.261	0.291	0.147
Fe^{2+}	0.260	0.259	0.243	0.269	0.272	0.242	0.281	0.287	0.280	0.277	0.265
Mn	0.006	0.006	0.006	0.007	0.005	0.006	0.005	0.005	0.004	0.005	0.006
Mg	0.729	0.728	0.793	0.706	0.705	0.774	0.667	0.650	0.679	0.646	0.756
Ca	0.900	0.876	0.876	0.884	0.885	0.879	0.887	0.873	0.877	0.899	0.889
K	0.000	0.000	0.005	0.004	0.002	0.000	0.003	0.000	0.000	0.004	0.001
Na	0.037	0.056	0.040	0.050	0.042	0.041	0.046	0.051	0.051	0.055	0.042
Wo	47.49	46.87	45.67	47.40	47.38	46.24	48.18	48.10	47.67	49.21	46.40
En	38.47	38.95	41.35	37.80	37.74	40.72	36.23	35.81	36.92	35.36	39.46
Fs	14.04	14.18	12.98	14.80	14.88	13.05	15.59	16.09	15.42	15.44	14.14

	P-15					P-19					
	c	*c*	*c*→	*b*	*c*	*c*→	*b*	*c*→	*b*	*c*→	*b*
SiO_2	44.92	45.60	47.76	49.79	48.78	50.98	51.01	49.50	50.94	50.70	49.87
TiO_2	3.17	3.16	2.01	1.33	1.91	1.43	1.47	0.80	0.59	0.57	1.78
Al_2O_3	6.63	7.05	5.01	3.87	4.51	3.52	2.84	7.69	5.93	5.92	3.00
FeO	9.92	9.15	8.22	6.69	8.10	7.37	8.41	5.39	5.29	5.16	9.05
MnO	0.22	0.10	0.15	0.14	0.15	0.15	0.23	0.16	0.15	0.09	0.24
MgO	12.36	12.30	14.03	15.11	13.79	14.52	14.55	15.50	16.66	16.40	13.44
CaO	21.52	21.66	21.91	21.61	22.12	22.13	21.25	20.08	19.05	19.89	20.79
K_2O	0.03	0.23	0.00	0.31	0.27	0.00	0.00	0.27	0.27	0.01	0.31
Na_2O	0.53	0.74	0.37	0.37	0.50	0.37	0.36	0.66	0.64	0.68	0.52
Total	99.30	99.98	99.47	99.22	100.11	100.48	100.11	100.05	99.53	99.41	98.99
Si	1.692	1.698	1.779	1.842	1.806	1.874	1.891	1.793	1.850	1.846	1.876
Ti	0.090	0.088	0.056	0.037	0.053	0.040	0.041	0.022	0.016	0.016	0.050
Al	0.294	0.309	0.220	0.169	0.197	0.153	0.124	0.328	0.254	0.254	0.133
Fe^{2+}	0.312	0.285	0.256	0.207	0.251	0.227	0.261	0.163	0.161	0.157	0.285
Mn	0.007	0.003	0.005	0.005	0.005	0.005	0.007	0.005	0.005	0.003	0.008
Mg	0.694	0.683	0.779	0.833	0.761	0.796	0.804	0.837	0.902	0.890	0.753
Ca	0.869	0.865	0.874	0.857	0.877	0.872	0.844	0.779	0.741	0.776	0.838
K	0.001	0.011	0.000	0.015	0.013	0.000	0.000	0.012	0.012	0.001	0.015
Na	0.039	0.054	0.027	0.027	0.036	0.026	0.026	0.046	0.045	0.048	0.038
Wo	46.17	47.11	45.66	45.06	46.30	45.89	44.05	43.67	40.96	42.50	44.48
En	36.88	37.20	40.70	43.80	40.18	41.89	41.96	46.92	49.86	48.74	39.97
Fs	16.95	15.69	13.64	11.15	13.52	12.21	13.99	9.42	9.18	8.76	15.55

	P-24						P-38				
	c→	*b*	*c*→	*b*	*c*→	*b*	mic	*c*→	*b*	*c*→	*b*
SiO_2	46.38	50.98	48.41	47.76	49.73	49.57	48.34	48.89	47.14	47.01	48.51
TiO_2	2.38	1.52	1.49	1.96	0.82	1.42	1.89	0.87	1.43	1.45	1.04
Al_2O_3	9.42	3.16	7.41	6.67	7.68	4.91	5.07	6.84	8.45	8.75	6.76
FeO	8.65	8.45	7.15	7.35	5.67	7.15	7.02	5.10	5.71	5.70	6.17
MnO	0.19	0.23	0.18	0.16	0.14	0.18	0.15	0.12	0.11	0.10	0.17
MgO	12.24	14.49	14.01	13.24	15.49	14.18	13.38	14.70	13.54	13.76	14.36
CaO	20.43	21.23	20.35	22.59	19.69	22.23	22.39	21.58	21.12	21.02	21.10
K_2O	0.03	0.00	0.00	0.00	0.02	0.02	0.00	0.00	0.00	0.00	0.00
Na_2O	0.90	0.39	0.75	0.41	0.74	0.36	0.48	0.67	0.65	0.73	0.76
Total	100.64	100.45	99.75	100.14	99.98	100.02	98.71	98.76	98.15	98.52	98.85
Si	1.708	1.884	1.784	1.767	1.810	1.832	1.814	1.806	1.760	1.746	1.796
Ti	0.066	0.042	0.041	0.055	0.022	0.039	0.053	0.024	0.040	0.040	0.029
Al	0.409	0.138	0.322	0.291	0.330	0.214	0.224	0.298	0.372	0.383	0.295
Fe^{2+}	0.267	0.261	0.220	0.227	0.173	0.221	0.220	0.157	0.178	0.177	0.191
Mn	0.006	0.007	0.006	0.005	0.004	0.006	0.005	0.004	0.003	0.003	0.005
Mg	0.672	0.798	0.770	0.730	0.840	0.781	0.748	0.809	0.754	0.762	0.793
Ca	0.806	0.841	0.804	0.896	0.768	0.880	0.900	0.854	0.845	0.836	0.837

(*continued on next page*)

Please cite this article in press as: Temel, A., et al. Alkaline series related to Early-Middle Miocene intra-continental rifting in a collision zone: An example from Polatlı, Central Anatolia, Turkey. Journal of Asian Earth Sciences (2010), doi:10.1016/j.jseaes.2009.12.017

Table 4 (*continued*)

K	0.064	0.028	0.054	0.029	0.052	0.026	0.035	0.048	0.047	0.052	0.054
Na	0.001	0.000	0.000	0.000	0.001	0.001	0.000	0.000	0.000	0.000	0.000
Wo	46.21	44.24	44.80	48.33	43.12	46.77	48.17	46.90	47.55	47.11	45.97
En	38.52	42.02	42.92	39.40	47.18	41.50	40.03	44.45	42.42	42.92	43.54
Fs	15.27	13.74	12.28	12.26	9.69	11.74	11.79	8.65	10.03	9.98	10.49

	P-38		P-41					P-42			
	c→	*b*	*c*→	*b*	mic	*c*→	*b*	*c*→	*b*	*c*→	*b*
SiO_2	46.43	46.50	46.59	46.78	47.42	48.45	46.70	51.10	50.39	46.60	46.58
TiO_2	2.05	1.86	1.99	1.65	1.66	1.41	2.04	0.96	1.11	2.17	2.11
Al_2O_3	9.43	8.68	10.10	9.64	9.40	7.52	9.93	3.88	4.70	7.52	7.68
FeO	7.30	6.93	5.94	6.30	5.68	6.71	6.76	5.30	6.06	6.68	6.68
MnO	0.15	0.11	0.16	0.12	0.12	0.19	0.15	0.14	0.15	0.13	0.08
MgO	12.32	12.97	12.82	12.94	13.37	14.26	12.66	15.47	14.68	13.00	13.01
CaO	20.64	20.77	20.00	19.79	20.38	18.71	19.02	23.36	22.85	23.32	23.37
K_2O	0.02	0.00	0.00	0.00	0.01	0.00	0.00	0.01	0.00	0.00	0.00
Na_2O	0.90	0.85	0.73	0.79	0.85	0.95	0.95	0.43	0.41	0.49	0.43
Total	99.24	98.66	98.32	98.00	98.88	98.19	98.22	100.65	100.36	99.91	99.94
Si	1.727	1.735	1.741	1.753	1.756	1.806	1.749	1.860	1.847	1.724	1.723
Ti	0.057	0.052	0.056	0.047	0.046	0.039	0.058	0.026	0.031	0.060	0.059
Al	0.413	0.381	0.445	0.426	0.410	0.330	0.438	0.167	0.203	0.328	0.335
Fe^{2+}	0.227	0.216	0.186	0.197	0.176	0.209	0.212	0.161	0.186	0.207	0.207
Mn	0.005	0.003	0.005	0.004	0.004	0.006	0.005	0.004	0.005	0.004	0.002
Mg	0.683	0.721	0.714	0.722	0.738	0.793	0.706	0.839	0.802	0.717	0.717
Ca	0.822	0.830	0.801	0.794	0.808	0.747	0.763	0.911	0.897	0.924	0.926
K	0.065	0.061	0.053	0.057	0.061	0.069	0.069	0.030	0.029	0.035	0.031
Na	0.001	0.000	0.000	0.000	0.000	0.000	0.000	0.000	0.000	0.000	0.000
Wo	47.47	46.97	47.09	46.35	46.94	42.73	45.40	47.66	47.60	50.01	50.06
En	39.42	40.80	41.99	42.14	42.85	45.32	42.02	43.90	42.54	38.80	38.76
Fs	13.11	12.22	10.92	11.51	10.21	11.96	12.59	8.44	9.86	11.18	11.18

	P-42		P-43					
	c→	*b*	*c*→	*b*	*c*→	*b*	*c*→	*b*
SiO_2	49.67	45.83	50.13	45.51	50.49	45.71	49.71	49.50
TiO_2	1.11	2.24	1.53	2.72	1.35	3.27	2.10	2.20
Al_2O_3	4.16	7.79	4.23	8.19	4.84	7.93	4.49	4.69
FeO	5.62	6.91	7.42	8.05	6.74	8.74	7.61	7.82
MnO	0.14	0.13	0.16	0.09	0.13	0.20	0.16	0.16
MgO	14.90	12.75	14.10	12.17	14.24	11.64	13.39	13.24
CaO	23.13	23.17	22.53	22.85	22.60	22.67	22.91	22.81
K_2O	0.00	0.01	0.00	0.00	0.03	0.00	0.01	0.01
Na_2O	0.38	0.48	0.48	0.47	0.47	0.61	0.59	0.55
Total	99.11	99.31	100.59	100.04	100.90	100.78	100.97	100.97
Si	1.841	1.708	1.845	1.693	1.847	1.696	1.829	1.823
Ti	0.031	0.063	0.042	0.076	0.037	0.091	0.058	0.061
Al	0.182	0.342	0.184	0.359	0.208	0.347	0.195	0.204
Fe^{2+}	0.174	0.215	0.228	0.250	0.206	0.271	0.234	0.241
Mn	0.004	0.004	0.005	0.003	0.004	0.006	0.005	0.005
Mg	0.823	0.708	0.773	0.675	0.777	0.644	0.734	0.727
Ca	0.918	0.925	0.888	0.911	0.886	0.901	0.903	0.900
K	0.027	0.035	0.034	0.034	0.034	0.044	0.042	0.039
Na	0.000	0.001	0.000	0.000	0.002	0.000	0.001	0.001
Wo	47.95	50.05	47.00	49.60	47.40	49.62	48.25	48.20
En	42.96	38.30	40.92	36.75	41.56	35.45	39.23	38.91
Fs	9.09	11.64	12.08	13.64	11.04	14.93	12.52	12.89

Abbrevations: mic: microlite; c: center; b: border; Wo: wollastonite; En: enstatite; Fs: ferrosillite.

(La_N/Yb_N = 3.08–11.43) (Thompson, 1982). All samples are characterized by almost flat patterns of REE from Dy to Lu relative to the LREE.

5.3. Sr–Nd Isotope geochemistry

Nine samples have been analysed for Sr and Nd isotopes and results are listed in Table 7. The isotopic compositions of $^{87}Sr/^{86}Sr$ ratios range from 0.703497 to 0.704964; $^{143}Nd/^{144}Nd$ ratios range from 0.512769 to 0.512980.

The variations in the $^{87}Sr/^{86}Sr$ and $^{143}Nd/^{144}Nd$ ratios of the Polatlı lavas are shown and compared with the bulk earth and the mantle array in Fig. 7. Most of the Polatlı lavas plot in the depleted quadrant of the mantle array with lesser amount of isotopically enriched samples. The Nd isotopic compositions are relatively enriched relatively to the bulk earth, whereas Sr isotopes of the great majority of the samples are depleted relative to the bulk earth with lesser amount of enriched samples relative to the bulk earth. Most samples plot within the mantle array.

The isotopic compositions of the Polatlı lavas are compared with those of a selection of volcanic suites worldwide. The comparison reveals that isotopic compositions of the Polatlı lavas range from isotopically depleted mantle (DM) to enriched mantle similar to Society Island lavas (Dewey et al., 1990), which is characterized by EMII components in their source regions (Zindler and Hart,

Please cite this article in press as: Temel, A., et al. Alkaline series related to Early-Middle Miocene intra-continental rifting in a collision zone: An example from Polatlı, Central Anatolia, Turkey. Journal of Asian Earth Sciences (2010), doi:10.1016/j.jseaes.2009.12.017

Table 5
Selected microprobe analyses of olivine. Number of cations on the basis of 4 oxygen.

	Olivine											
	P-1						P-15					
	c→	*b*	*c*→	*b*	*c*→	*b*	*c*→	*b*	*c*→	*b*	*c*→	*b*
SiO_2	37.22	37.07	36.73	35.96	37.22	37.68	38.42	39.34	39.08	38.12	36.43	38.79
TiO_2	0.00	0.00	0.08	0.04	0.00	0.00	0.00	0.05	0.00	0.00	0.03	0.04
Al_2O_3	0.01	0.05	0.04	0.02	0.04	0.03	0.00	0.04	0.05	0.04	0.00	0.06
MnO	0.58	0.59	0.66	0.85	0.48	0.55	0.29	0.37	0.31	0.44	0.51	0.23
MgO	36.94	35.61	33.72	31.29	37.97	35.33	41.12	42.30	43.22	39.16	32.59	44.62
CaO	0.29	0.44	0.57	0.46	0.33	0.40	0.68	0.26	0.38	0.46	0.61	0.46
Fe_2O_3	2.37	2.11	1.89	1.93	2.37	0.59	1.19	0.00	1.45	0.96	0.94	2.37
FeO	23.28	25.00	27.35	29.73	21.51	26.33	17.96	17.12	16.30	20.79	28.19	13.59
Total	100.44	100.65	100.85	100.08	99.70	100.86	99.54	99.47	100.64	99.86	99.21	99.93
Si	0.9764	0.9783	0.9788	0.9790	0.9760	0.9938	0.9884	1.0055	0.9856	0.9899	0.9898	0.9759
Ti	0.0000	0.0000	0.0015	0.0009	0.0000	0.0000	0.0000	0.0009	0.0000	0.0000	0.0006	0.0007
Al	0.0004	0.0015	0.0014	0.0007	0.0012	0.0009	0.0001	0.0011	0.0014	0.0013	0.0000	0.0019
Fe2	0.5107	0.5517	0.6094	0.6768	0.4716	0.5808	0.3863	0.3797	0.3438	0.4515	0.6405	0.2859
Fe3	0.0468	0.0419	0.0380	0.0395	0.0468	0.0116	0.0230	−0.014	0.0275	0.0188	0.0193	0.0449
Mn	0.0128	0.0131	0.0149	0.0195	0.0107	0.0123	0.0062	0.0080	0.0066	0.0096	0.0116	0.0049
Mg	1.4448	1.4010	1.3397	1.2702	1.4843	1.3893	1.5772	1.6115	1.6250	1.5161	1.3203	1.6735
Ca	0.0081	0.0124	0.0163	0.0134	0.0093	0.0114	0.0187	0.0072	0.0102	0.0128	0.0179	0.0123
Fo	71.70	69.78	66.92	63.32	73.72	69.67	79.14	81.17	81.13	75.96	66.29	83.29
Fa	27.67	29.57	32.34	35.71	25.75	29.71	20.54	18.42	18.54	23.56	33.13	16.47
	P-19						P-24					
	c→	*b*	*c*→	*b*	*c*	*c*	*c*→	*b*	*c*→	*b*	*c*	*c*
SiO_2	39.24	39.06	39.64	39.46	36.02	37.33	39.41	39.50	40.44	39.57	39.31	39.13
TiO_2	0.04	0.00	0.00	0.00	0.00	0.15	0.00	0.00	0.06	0.03	0.00	0.00
Al_2O_3	0.04	0.05	0.04	0.08	0.02	0.21	0.03	0.07	0.08	0.05	0.00	0.04
MnO	0.26	0.22	0.22	0.22	0.64	0.65	0.22	0.29	0.23	0.24	0.35	0.25
MgO	43.69	44.43	43.98	44.98	31.32	27.47	41.52	41.40	45.90	43.90	40.40	42.22
CaO	0.20	0.36	0.28	0.57	0.23	0.49	0.26	0.21	0.29	0.22	0.21	0.25
Fe_2O_3	1.25	1.64	0.00	1.31	1.78	0.00	0.00	0.00	0.00	0.93	0.00	0.56
FeO	16.10	14.29	15.87	13.88	30.18	33.51	18.86	20.14	13.89	16.36	20.66	18.03
Total	100.69	99.88	100.03	100.37	100.00	99.81	100.31	101.61	100.89	101.21	100.94	100.43
Si	0.9868	0.9838	0.9993	0.9864	0.9815	1.0396	1.0056	0.9991	1.0015	0.9900	1.0051	0.9941
Ti	0.0008	0.0000	0.0000	0.0000	0.0000	0.0032	0.0000	0.0000	0.0012	0.0006	0.0000	0.0000
Al	0.0011	0.0014	0.0013	0.0024	0.0005	0.0068	0.0010	0.0020	0.0024	0.0013	0.0000	0.0012
Fe2	0.3385	0.3010	0.3344	0.2901	0.6878	0.8727	0.4145	0.4262	0.2956	0.3422	0.4518	0.3829
Fe3	0.0237	0.0311	0.0000	0.0247	0.0365	−0.092	−0.012	−0.000	−0.007	0.017	−0.010	0.0106
Mn	0.0056	0.0047	0.0046	0.0047	0.0147	0.0153	0.0048	0.0062	0.0048	0.0051	0.0075	0.0054
Mg	1.6381	1.6684	1.6527	1.6764	1.2723	1.1402	1.5792	1.5609	1.6947	1.6373	1.5399	1.5990
Ca	0.0054	0.0096	0.0076	0.0152	0.0068	0.0146	0.0070	0.0057	0.0076	0.0059	0.0059	0.0068
Fo	81.66	83.20	82.98	83.99	63.26	58.90	79.50	78.32	85.28	81.78	77.42	80.03
Fa	18.06	16.56	16.79	15.77	36.01	40.31	20.25	21.37	14.48	17.97	22.20	19.70
	P-41						P-42					
	c→	*b*	*c*→	*b*	*c*→	*b*	*c*→	*b*	*c*→	*b*	*c*→	*b*
SiO_2	39.60	38.59	39.88	38.54	39.50	38.57	39.32	38.49	40.06	40.21	33.95	38.15
TiO_2	0.03	0.00	0.00	0.00	0.01	0.03	0.05	0.09	0.06	0.00	0.01	0.00
Al_2O_3	0.05	0.02	0.04	0.06	0.06	0.03	0.04	0.05	0.06	0.03	0.02	0.07
MnO	0.23	0.55	0.23	0.39	0.17	0.55	0.48	0.46	0.20	0.17	0.31	0.47
MgO	43.41	37.54	45.02	39.67	43.72	39.20	39.86	38.71	46.25	45.27	35.44	38.66
CaO	0.23	0.17	0.21	0.25	0.20	0.25	0.31	0.42	0.19	0.26	0.30	0.37
Fe_2O_3	0.00	0.00	0.00	0.00	0.00	0.00	0.00	0.00	0.16	0.00	2.21	0.42
FeO	15.47	21.66	13.31	19.43	14.43	20.09	20.65	21.63	13.13	14.68	18.34	21.62
Total	99.02	98.52	98.68	98.34	98.09	98.70	100.69	99.85	100.10	100.61	90.34	99.71
Si	1.0087	1.0214	1.0090	1.0090	1.0113	1.0097	1.0097	1.0018	0.9966	1.0016	0.9757	0.9948
Ti	0.0005	0.0000	0.0000	0.0000	0.0002	0.0006	0.0009	0.0017	0.0011	0.0000	0.0002	0.0000
Al	0.0016	0.0005	0.0011	0.0019	0.0018	0.0008	0.0012	0.0016	0.0017	0.0009	0.0006	0.0022
Fe2	0.3495	0.5228	0.3006	0.4453	0.3337	0.4613	0.4658	0.4796	0.2732	0.3100	0.4407	0.4713
Fe3	−0.020	−0.043	−0.019	−0.020	−0.024	−0.022	−0.023	−0.008	0.0030	−0.004	0.0477	0.0082
Mn	0.0050	0.0124	0.0048	0.0086	0.0037	0.0122	0.0103	0.0101	0.0042	0.0035	0.0075	0.0104
Mg	1.6485	1.4815	1.6980	1.5481	1.6687	1.5299	1.5261	1.5023	1.7153	1.6813	1.5185	1.5029
Ca	0.0062	0.0048	0.0056	0.0071	0.0054	0.0070	0.0084	0.0116	0.0050	0.0068	0.0091	0.0102
Fo	83.13	75.08	85.57	78.11	84.22	77.20	77.09	75.75	85.95	84.46	75.38	75.41
Fa	16.62	24.30	14.19	21.46	15.59	22.19	22.39	23.74	13.84	15.36	24.25	24.06

(*continued on next page*)

Please cite this article in press as: Temel, A., et al. Alkaline series related to Early-Middle Miocene intra-continental rifting in a collision zone: An example from Polatlı, Central Anatolia, Turkey. Journal of Asian Earth Sciences (2010), doi:10.1016/j.jseaes.2009.12.017

Table 5 (*continued*)

	P-43				
	c	*c*→	*b*	*c*→	*b*
SiO_2	38.21	40.79	39.02	38.05	38.14
TiO_2	0.03	0.00	0.00	0.02	0.01
Al_2O_3	0.04	0.07	0.04	0.05	0.02
MnO	0.53	0.16	0.33	0.53	0.46
MgO	36.50	47.97	38.49	36.53	37.57
CaO	0.35	0.18	0.26	0.30	0.26
Fe_2O_3	0.00	0.00	0.00	0.28	0.98
FeO	24.78	11.05	22.39	25.15	23.92
Total	100.45	100.21	100.53	100.87	101.26
Si	1.0034	1.0035	1.0116	0.9961	0.9900
Ti	0.0007	0.0000	0.0000	0.0004	0.0002
Al	0.0012	0.0019	0.0012	0.0015	0.0005
Fe2	0.5536	0.2364	0.5096	0.5505	0.5191
Fe3	−0.009	−0.009	−0.024	0.0055	0.0191
Mn	0.0118	0.0033	0.0073	0.0118	0.0102
Mg	1.4290	1.7592	1.4875	1.4259	1.4537
Ca	0.0097	0.0046	0.0072	0.0083	0.0072
Fo	71.99	88.41	75.12	71.52	72.61
Fa	27.42	11.43	24.51	27.89	26.88

Abbrevations: mic: microlite; c: center; b: border; Fo: forstherite; Fa: fayalite.

Table 6
Selected microprobe analyses of Ti-oxides. Number of cations on the basis of 24 oxygen.

	Ti-magnetite										
	P-1				P-7			P-15			
	c	c	c	c	c	c	c	c	c	c	c
SiO_2	0.15	0.19	0.03	0.08	0.00	0.11	0.09	0.03	0.05	0.07	0.03
Al_2O_3	2.05	1.64	1.73	1.83	0.93	0.78	0.72	1.31	1.09	1.31	1.38
FeOt	69.44	69.51	70.50	69.95	67.93	85.19	82.37	69.14	67.87	69.25	70.13
MgO	2.42	2.83	2.77	3.14	2.52	3.18	3.82	2.47	2.48	2.69	2.60
CaO	0.00	0.00	0.00	0.00	0.23	0.18	0.26	0.37	0.34	0.16	0.00
TiO_2	23.49	24.53	23.22	23.68	24.65	6.08	8.12	24.76	25.97	24.79	24.26
MnO	0.77	0.90	0.73	0.78	0.22	0.81	1.16	0.85	0.76	0.78	0.79
Total	98.32	99.60	98.98	99.46	96.47	96.34	96.54	98.93	98.56	99.05	99.18
Si	0.029	0.036	0.006	0.015	0	0.02	0.017	0.006	0.009	0.014	0.005
Al	0.469	0.37	0.392	0.411	0.217	0.179	0.165	0.298	0.25	0.298	0.312
Fe^{3+}	8.623	8.502	8.89	8.758	8.406	13.816	13.297	8.482	8.127	8.484	8.652
Fe^{2+}	2.629	2.613	2.444	2.4	2.856	0	0	2.677	2.899	2.666	2.638
Mg	0.7	0.806	0.793	0.891	0.743	0.919	1.1	0.711	0.718	0.772	0.747
Ca	0	0	0	0	0.048	0.038	0.054	0.077	0.07	0.032	0
Ti	3.423	3.527	3.356	3.397	3.674	0.887	1.179	3.593	3.794	3.589	3.511
Mn	0.126	0.145	0.119	0.127	0.036	0.133	0.19	0.139	0.126	0.128	0.129

	P-19				P-24			P-43		
	c	c	c	c	c	c	c	c	c	c
SiO_2	0.16	0.15	0.11	0.13	0.07	0.39	0.10	0.03	0.08	0.06
Al_2O_3	1.54	1.44	1.45	1.30	1.90	1.83	1.34	1.69	1.44	1.43
FeOt	68.19	64.12	63.85	63.66	63.39	61.20	63.77	68.04	69.32	69.27
MgO	1.99	2.82	2.94	2.83	1.94	2.30	2.09	2.14	1.27	1.45
CaO	0.39	0.21	0.32	0.16	0.12	0.02	0.08	0.14	0.22	0.08
TiO_2	23.43	26.62	27.42	27.65	27.29	28.42	26.31	24.46	24.06	24.28
MnO	0.80	0.77	0.62	0.81	0.71	0.72	0.84	0.94	0.90	0.81
Total	96.50	96.14	96.72	96.54	95.42	94.88	94.53	97.43	97.28	97.38
Si	0.031	0.031	0.021	0.025	0.015	0.079	0.021	0.006	0.015	0.012
Al	0.359	0.336	0.336	0.303	0.45	0.435	0.321	0.391	0.336	0.333
Fe^{3+}	8.571	7.647	7.468	7.384	7.277	6.774	7.636	8.382	8.486	8.433
Fe^{2+}	2.715	2.989	3.046	3.138	3.391	3.567	3.187	2.792	2.997	3.022
Mg	0.586	0.835	0.864	0.835	0.581	0.692	0.633	0.625	0.375	0.426
Ca	0.083	0.045	0.067	0.034	0.026	0.005	0.018	0.029	0.047	0.016
Ti	3.487	3.971	4.061	4.11	4.129	4.317	4.015	3.611	3.583	3.611
Mn	0.134	0.129	0.104	0.136	0.121	0.124	0.144	0.156	0.15	0.136

Abbreviations: c: center.

1986) and fall into the field of Galatian volcanic rocks from Central Turkey that were derived from a lithospheric mantle metasomatized with an ancient subduction event (Varol Muratçay, 2006). According to this diagram, the slight enrichment in Sr isotope ratios in Polatlı lavas can be attributed to addition of crustal components.

6. Discussion

6.1. Source characteristics

In order to determine the geotectonic environment of the Polatlı lavas, trace element contents of the basaltic samples are plotted on

Please cite this article in press as: Temel, A., et al. Alkaline series related to Early-Middle Miocene intra-continental rifting in a collision zone: An example from Polatlı, Central Anatolia, Turkey. Journal of Asian Earth Sciences (2010), doi:10.1016/j.jseaes.2009.12.017

Table 7
Major-oxide, trace, rare earth element and Sr–Nd isotope analysis of representative samples from Polatlı volcanic rocks.

	P-1	P-2	P-3	P-6	P-8	P-9	P-10	P-11	P-12	P-13	P-14
wt.%											
SiO_2	46.84	49.67	46.29	45.94	46.65	45.38	47.11	46.08	44.71	45.04	45.95
Al_2O_3	18.2	17.65	18.03	16.93	17.95	17.19	16.64	16.97	16.62	15.92	16.18
Fe_2O_3	9.98	9.68	9.91	9.52	10.24	10.07	8.83	9.13	9.38	10.13	9.95
MnO	0.157	0.104	0.155	0.155	0.107	0.159	0.15	0.139	0.143	0.156	0.158
MgO	4.95	3.01	4.96	5.36	4.34	6.71	5.75	5.72	6.69	8.2	7.98
CaO	8.66	8.82	8.36	8.98	10.85	10.27	8.51	10.22	10.09	9.93	11.1
Na_2O	3.83	3.94	4.03	4.49	3.12	3.59	4.04	3.42	4.25	3.72	3.46
K_2O	1.78	1.33	1.76	1.23	0.84	0.94	2	1.61	1.24	1.31	1.35
TiO_2	2.04	1.65	2.05	1.62	2.05	2.01	1.83	1.8	1.74	1.72	1.59
P_2O_5	0.54	0.55	0.51	0.58	0.32	0.28	0.51	0.48	0.39	0.41	0.48
LOI	3.95	3.93	4.34	4.52	4.52	3.18	4.95	4.35	4.4	2.47	2.08
Total	100.93	100.34	100.4	99.34	100.98	99.77	100.32	99.92	99.65	99	100.28
ppm											
Nb	25.3	27.6	25.5	28.2	16.9	16.5	37.6	24.6	21.8	18.8	20.8
Zr	225.5	212.8	230.9	200.5	165.6	170.5	212.8	185.9	166.3	164.6	155
Y	27.4	26	27	24.6	27.6	28.1	27.4	25.7	23.2	24.2	22.9
Sr	931.7	1121.1	978	977.3	498.9	520	684.2	755.8	783.3	898.7	787
Rb	31.3	6.3	33.6	8.1	9.9	11.4	32.3	27.6	19.6	19.9	21.8
Ga	24.2	21.7	24.9	19.3	23.4	24	24.2	20.2	19.7	19.6	17.5
Ni	16.6	59.6	16.5	53.5	57	50.8	80.6	71.3	68	138	129
Co	36.3	32	43.1	34.6	42.1	42.5	33.8	37.3	38.3	42.5	41.3
Cr	3.8	75.3	5.7	56.9	81.9	78.7	160.2	114.3	80.2	247.2	227.9
V	171.2	160.4	183.2	159.1	187.6	190.3	162	179	166.3	161.4	163.4
Ba	430.5	584.9	413.9	471.2	110.7	114.4	641	361.5	298.8	330	375.2
La	28.07	na	na	na	na	na	na	na	na	na	na
Ce	59.71	na	na	na	na	na	na	na	na	na	na
Pr	7.06	na	na	na	na	na	na	na	na	na	na
Nd	28.2	na	na	na	na	na	na	na	na	na	na
Sm	5.34	na	na	na	na	na	na	na	na	na	na
Eu	1.8	na	na	na	na	na	na	na	na	na	na
Gd	5.45	na	na	na	na	na	na	na	na	na	na
Tb	0.77	na	na	na	na	na	na	na	na	na	na
Dy	4.48	na	na	na	na	na	na	na	na	na	na
Ho	0.87	na	na	na	na	na	na	na	na	na	na
Er	2.36	na	na	na	na	na	na	na	na	na	na
Tm	0.37	na	na	na	na	na	na	na	na	na	na
Yb	2.29	na	na	na	na	na	na	na	na	na	na
Lu	0.37	na	na	na	na	na	na	na	na	na	na
Hf	4.07	na	na	na	na	na	na	na	na	na	na
Ta	1.38	na	na	na	na	na	na	na	na	na	na
Pb	4.57	na	na	na	na	na	na	na	na	na	na
Th	3.27	na	na	na	na	na	na	na	na	na	na
U	0.98	na	na	na	na	na	na	na	na	na	na
$^{87}Sr/^{86}Sr$	0.7043	na	na	na	na	na	na	na	na	na	na
$^{143}Nd/^{144}Nd$	0.5128	na	na	na	na	na	na	na	na	na	na

	P-15	P-16	P-17	P-18	P-19	P-20	P-21	P-24	P-38	P-39	P-40
wt.%											
SiO_2	47.14	46.79	46.73	45.22	49.14	48.29	46.31	48.07	48.56	47.78	48.93
Al_2O_3	17.45	16.94	16.81	17.22	16.81	16.36	15.25	17.11	16.7	16.01	16.74
Fe_2O_3	9.79	10.22	10.33	9.83	10.03	9.74	8.78	9.69	9.76	9.31	8.36
MnO	0.153	0.148	0.163	0.152	0.164	0.167	0.149	0.154	0.172	0.134	0.142
MgO	6.94	6.23	6.55	6.28	5.55	5.4	7.75	5.31	4.34	5.62	5.47
CaO	9.93	9.2	9.7	9.84	9.24	9.49	10.25	8.93	9.82	10.09	7.27
Na_2O	4.27	3.56	3.56	2.48	3.67	3.27	3.31	3.37	2.91	3.55	4.39
K_2O	1.49	1.27	1.13	1.14	1.5	1.56	1.07	1.49	1.65	1.61	2.27
TiO_2	1.83	1.95	1.9	1.89	1.78	1.76	1.43	1.75	1.72	1.62	1.59
P_2O_5	0.41	0.41	0.37	0.3	0.34	0.33	0.62	0.38	0.46	0.44	0.47
LOI	1	3.37	3.24	5	2.14	4.4	4.17	2.53	2.79	2.82	3.35
Total	100.39	100.1	100.49	99.33	100.36	100.75	99.08	98.78	98.87	98.98	98.96
ppm											
Nb	20.5	23.8	20	16.5	23.9	24	na	18.78	22.49	na	na
Zr	170.5	173.6	166.5	174.4	176	169.1	na	168.43	148.19	na	na
Y	25.6	25.5	24.3	26	27.7	25.3	na	22.1	21.76	na	na
Sr	695.4	569.4	612.4	515.2	499.2	483.2	na	583.06	663.97	na	na
Rb	21.3	19.2	13.8	13.8	25.1	29.8	na	21.14	27.11	na	na
Ga	21.4	22.6	21.5	21.8	22.3	20.9	na	na	na	na	na
Ni	65.5	58.8	65.5	43.7	68.2	76.2	na	na	na	na	na
Co	43.6	37.8	40.5	37.9	37.6	42.4	na	na	na	na	na
Cr	79.4	142.9	156.5	57	126.3	156.2	na	na	na	na	na

(*continued on next page*)

Please cite this article in press as: Temel, A., et al. Alkaline series related to Early-Middle Miocene intra-continental rifting in a collision zone: An example from Polatlı, Central Anatolia, Turkey. Journal of Asian Earth Sciences (2010), doi:10.1016/j.jseaes.2009.12.017

Table 7 (*continued*)

V	172.4	168.4	176.3	151.1	160.6	152.4	na	na	na	na	na
Ba	304.7	247.2	204.1	139.8	445.8	287.2	na	247.73	516.03	na	na
La	21.07	na	na	na	16.69	na	na	19.52	20.05	na	na
Ce	45.05	na	na	na	36.17	na	na	42.28	42.58	na	na
Pr	5.41	na	na	na	4.48	na	na	5.15	5.15	na	na
Nd	22.19	na	na	na	19.34	na	na	21.67	21.43	na	na
Sm	4.57	na	na	na	4.45	na	na	4.66	4.51	na	na
Eu	1.59	na	na	na	1.62	na	na	1.59	1.6	na	na
Gd	5.05	na	na	na	5.1	na	na	5.07	4.93	na	na
Tb	0.73	na	na	na	0.78	na	na	0.75	0.72	na	na
Dy	4.4	na	na	na	4.73	na	na	4.54	4.32	na	na
Ho	0.86	na	na	na	0.93	na	na	0.89	0.84	na	na
Er	2.35	na	na	na	2.61	na	na	2.42	2.32	na	na
Tm	0.37	na	na	na	0.41	na	na	0.39	0.36	na	na
Yb	2.26	na	na	na	2.53	na	na	2.37	2.23	na	na
Lu	0.35	na	na	na	0.41	na	na	0.38	0.36	na	na
Hf	3.24	na	na	na	3.7	na	na	3.84	3.38	na	na
Ta	1.17	na	na	na	1.33	na	na	1.3	1.42	na	na
Pb	4.27	na	na	na	2.92	na	na	3.29	2.94	na	na
Th	2.03	na	na	na	2.32	na	na	2.37	2.44	na	na
U	0.63	na	na	na	0.6	na	na	0.69	0.98	na	na
$^{87}Sr/^{86}Sr$	0.704	na	na	na	0.704	na	na	0.7044	0.7042	na	na
$^{143}Nd/^{144}Nd$	0.5128	na	na	na	0.5128	na	na	0.5128	0.5129	na	na

	P-41	P-42	P-43	P-44	BCR-1[ϕ]
wt.%					
SiO_2	49.16	45.34	46.88	46.65	54.54
Al_2O_3	16.82	15.14	17.07	16.92	13.52
Fe_2O_3	8.41	9.07	9.78	9.75	13.50
MnO	0.137	0.144	0.152	0.149	0.18
MgO	5.71	7.89	6.4	6.55	3.50
CaO	7.29	10.27	9.07	9.16	6.99
Na_2O	4.26	3.64	3.65	3.31	3.29
K_2O	2.35	1.14	1.84	1.81	1.71
TiO_2	1.59	1.48	1.68	1.69	2.28
P_2O_5	0.46	0.54	0.6	0.62	0.36
LOI	2.61	4.35	1.82	2.05	
Total	98.79	99.01	98.93	98.67	
BHVO-1 (ppm)*					
Nb	38.1	20.93	23.01	na	16.62
Zr	150.62	142.63	160.1	na	159.35
Y	18.65	19.28	18.59	na	22.61
Sr	562.01	914.52	806.01	na	365.05
Rb	17.39	8.86	21.73	na	8.76
Ga	na	na	na	na	
Ni	na	na	na	na	
Co	na	na	na	na	
Cr	na	na	na	na	
V	na	na	na	na	
Ba	546.49	460.28	460.18	na	123.48
La	23.62	34.28	32.4	na	15.13
Ce	47.03	71.02	68.35	na	37.74
Pr	5.43	8.05	7.88	na	5.22
Nd	21.95	30.9	30.55	na	24.48
Sm	4.37	5.31	5.45	na	5.83
Eu	1.6	1.68	1.72	na	2.04
Gd	4.6	5.25	5.44	na	6.30
Tb	0.65	0.7	0.72	na	0.91
Dy	3.81	4.05	4.23	na	5.16
Ho	0.74	0.78	0.79	na	0.93
Er	2.03	2.12	2.17	na	2.35
Tm	0.33	0.33	0.34	na	0.34
Yb	2	2	2.06	na	1.95
Lu	0.32	0.32	0.33	na	0.29
Hf	3.55	3.25	3.54	na	4.52
Ta	2.36	1.25	1.37	na	1.36
Pb	3.08	5.09	5.1	na	4.88
Th	3.9	3.27	3	na	1.08
U	1.21	1.11	0.92	na	0.38
$^{87}Sr/^{86}Sr$	0.705	0.7047	0.7035	na	
$^{143}Nd/^{144}Nd$	0.5128	0.5130	0.5130	na	

Total iron is expressed as Fe_2O_3; wt.%: weight percent; LOI: loss on ignition; na: not analysed; [ϕ]BCR-1 and *BHVO-1 (international rock standards).

the Ti/100–Zr*3–Y ternary diagram of Pearce and Cann (1973). It is apparent from the Fig. 8 that Polatlı lavas appear to be derived from a source similar to the within-plate basalts. Furthermore, the ternary plots of Th–Hf/3–Ta (Menzies et al.,1991) is also used to distinguish the source regions of Polatlı lavas (Fig. 9). They have Th–Hf–Ta systematic consistent with the derivation from a source similar to within-plate basalts. Trace elements ratios such as Nb/La–Ba/La, Th/Yb–Ta/Yb and Zr/Nb–Y/Nb may be useful to assess the role of source component(s) (Pearce, 1983; Edwards et al., 1991; Alıcı et al., 1998, 2002; Temel et al., 1998a). The Ba/La and

Please cite this article in press as: Temel, A., et al. Alkaline series related to Early-Middle Miocene intra-continental rifting in a collision zone: An example from Polatlı, Central Anatolia, Turkey. Journal of Asian Earth Sciences (2010), doi:10.1016/j.jseaes.2009.12.017

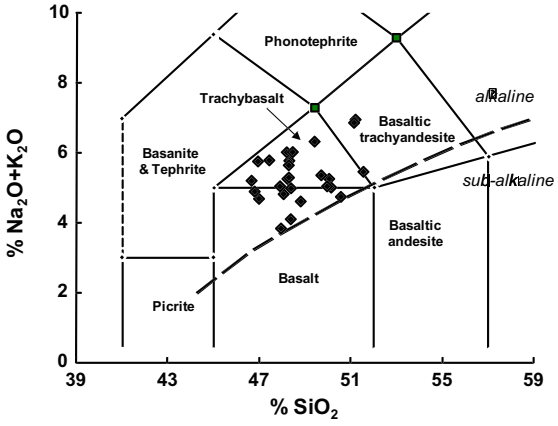

Fig. 3. Total alkali vs. silica diagram of the Polatlı volcanic rocks (Le Bas et al., 1986) The alkaline–subalkaline dividing line is from Miyashiro (1978).

Nb/La diagram (Fig. 10) has been used to distinguish the intra-plate basalt from the subduction-related basalts, since high Ba/Nb > 28 and Nb/La > 1 are the specific characteristics of island-arc magmas and intra-plate magmas, respectively. According to these criterion, low Ba/Nb and relatively high Nb/La ratios in Polatlı lavas can not be attributed to subduction processes. This is also supported by their low Ba/Ta ratios (<368). Thus, low Nb and Ta concentrations in the Polatlı lavas relative to the LIL elements in the spidergrams can be explained by the effects of crustal contamination rather than subduction processes. The trace element ratios of Polatlı lavas were compared with those of a selection of volcanic suites related to within-plate volcanism. The comparison reveals that the Nb/La and Ba/La ratios of the most of the Polatlı lavas are similar to Erciyes alkaline basalts (EAB, Kürkcüoğlu et al., 1998), Zuni-Bandera alkaline basalts (ZBAB, Menzies et al., 1991) and OIB.

The Th/Yb vs. Ta/Yb discrimination diagram has been used to distinguish basaltic rocks associated to within-plate source regions and subduction-related source regions (Pearce, 1983) (Fig. 11). Basalts derived from the convecting upper mantle (MORB), asthenosphere and lithosphere enriched from small volume partial melts all plot within or close to the mantle array (Pearce et al., 1990). It is apparent from the Fig. 11 that the great majority of the Polatlı lavas plot on the mantle array and OIB field (Chen and Frey, 1985; Chen et al., 1990; Gerlach et al., 1988; Chaffey et al., 1989; Gautier et al., 1990), confirming the suggestion from trace element chemistry that the source region(s) of Polatlı lavas had no subduction signatures. Moreover, some of the Polatlı lavas plot close to the EAB, RSAB (Red Sea alkaline basalts, Altherr et al., 1988), ZBAB and ZBTB (Zuni-Bandera Tholeiitic basalts, Menzies et al., 1991) fields which are typically originated from within-plate source region(s). It is clear from the Fig. 8 that Polatlı lavas generally scattered along the within-plate enrichment trend rather than subduction zone enrichment trend.

On a Zr/Nb vs. Y/Nb diagram (Fig. 12), OIB-like asthenospheric melts have low Zr/Nb and Y/Nb ratios. Furthermore, mantle melts show a positive correlation with the highest degree of partial melts having the highest Zr/Nb and Y/Nb ratios. Demonstrate that, Polatlı lavas clearly plot within in ZBAB and EAB fields which were generated from asthenopheric mantle. According to this diagram, Polatlı lavas have also Zr/Nb and Y/Nb ratios similar to OIB-like asthenospheric magmas but their variations in these ratios should be due to different degree of partial melting. It could be said that all the Polatlı lavas were derived from the same asthenospheric mantle source via variable degree of partial melting.

La/Yb ratio in a mafic lavas is controlled by garnet and may be determine the source characteristics of Polatlı lavas. Since Yb is compatible in garnet and, low La/Yb ratios can be attributed to the presence of residual garnet-bearing mantle source as expected in OIBs. La vs. La/Yb diagram (Fig. 13) was carried out to determine the source mineralogy of Polatlı lavas and record the degrees of partial melting. Shaw's (1970) fractional and batch melting equations were used for the modelling. La and Yb concentrations of garnet–peridotite are 2.1 and 1.1, respectively (Frey, 1980). The modal mineralogy of the garnet–peridotite is 63% olivine, 82% orthopyroxene, 30% clinopyroxene and 5% garnet (Wilson, 1989). Mineral/melt (K_d) partition coefficients of the basaltic melts are from Irving and Frey (1978), Fujimaki et al. (1984) and Rollinson (1993). It is further calculated from the K_d values of the basaltic melts and modal mineralogy of the garnet–peridotite that the bulk partition coefficient for La is $D_{La} = 0.0054$ and for Yb is $D_{Yb} = 0.3348$. It is apparent from Fig. 13 that the Polatlı lavas clearly plot on the batch melting curve of garnet–peridotite. This indicates an OIB-like mantle source with residual garnet signatures and partial melting of garnet–peridotite is the major source in the genesis of Polatlı lavas. Moreover, Polatlı lavas have experienced variable degrees of partial melting. Modelling indicates that all the Polatlı lavas were generated from the same OIB-like asthenopheric mantle via degree of partial meting ranging from ~5% to ~20%.

Generally, Polatlı lavas have trace element abundance patterns and Th/Y (0.04–0.21), Nb/Y (0.59–2.04), Ba/Nb (6.55–22.94), La/Nb (0.62–1.64), Th/Nb (0.06–0.20) and Rb/Nb (0.23–1.32) ratios almost similar to OIB (Edwards et al., 1991; Temel et al., 1998a, 2000). Nevertheless, they have relatively depleted HFS elements ratios relative to the OIB. Moreover, slight negative Nb and Ta anomalies relative to other trace elements and some relatively high $^{87}Sr/^{86}Sr$ isotope ratios can be attributed to the effects of crustal contamination in their evolution. Nonetheless, the partial melting process, which is supported by the variations in Zr/Nb and Y/Nb ratios and REE-modelling studies, is also effective in the genesis of Polatlı lavas. The Zr/Nb ratio strongly depends on the amount of clinopyroxene in the residue. Hence, the Zr/Nb and Y/Nb ratios increase with increasing degree of partial melting.

Ratio-ratio plots and REE modelling demonstrate that Polatlı lavas have compositions consistent with derivation from the OIB-like asthenospheric mantle similar to other within-plate volcanisms such as EAB, and RSAB. Consequently, geochemical studies demonstrate that Polatlı lavas derived from a same asthenospheric mantle and experienced variable degree of partial melting, since geochemical variations, especially in Zr/Nb and Y/Nb, are due to different degree of partial melting rather than source heterogeneities.

7. Possible source of the Polatlı volcanites

We do not find any field evidence for the volcanic emission centres and/or the tectonic lines that produced the Polatlı lavas, possibly due to the shortening deformation and erosion that followed the Miocene extensional period. There are, however, some field observations (Demirbağ, 2005) that suggest the flow direction of these basaltic rocks. Thicknesses of lava flows, estimated to ca. 80 m at the south (Yurtyeri, 1989) (Fig. 1) decrease to ca. 15 m at the northern sections (Akdağ, 2005). Thicknesses of the baked zones developed in the underlying clastics also progressively decrease northwards, from ca. 50 cm. at the southern to ca. 8 cm at the northern sections (Fig. 1). We interpret this difference as due to the fact that the northern clastics were heated by gradually decreasing quantities of volcanics, the temperature and the cooling duration to which these sedimentary rocks were exposed also decreasing away from the emission centers. We thus think that lavas erupted from a southern source and flowed towards the north. This southern possible source is near to the Eskişehir fault zone, an

Please cite this article in press as: Temel, A., et al. Alkaline series related to Early-Middle Miocene intra-continental rifting in a collision zone: An example from Polatlı, Central Anatolia, Turkey. Journal of Asian Earth Sciences (2010), doi:10.1016/j.jseaes.2009.12.017

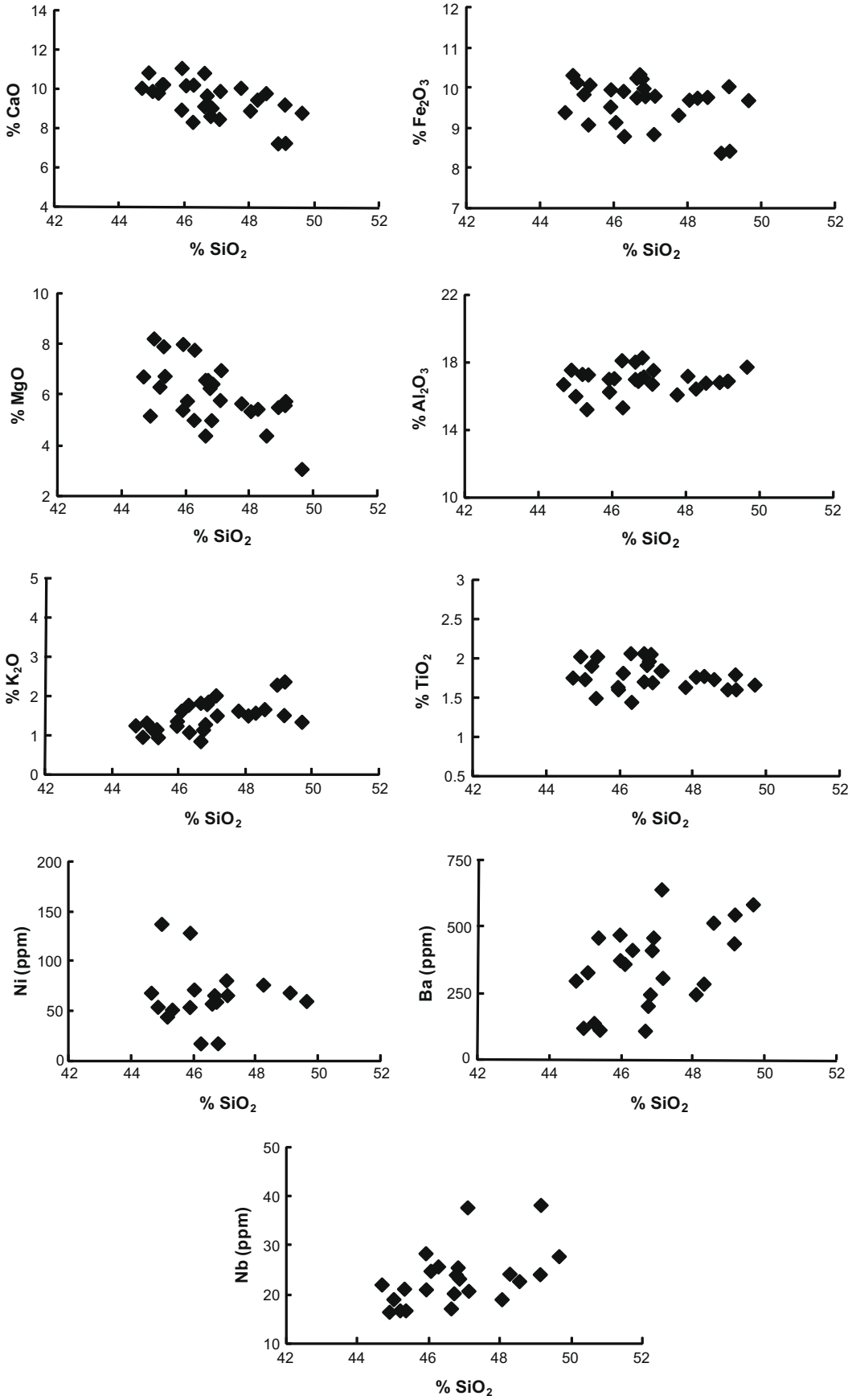

Fig. 4. SiO_2 variation diagrams for selected major-oxides and trace elements of the Polatlı volcanic rocks.

Please cite this article in press as: Temel, A., et al. Alkaline series related to Early-Middle Miocene intra-continental rifting in a collision zone: An example from Polatlı, Central Anatolia, Turkey. Journal of Asian Earth Sciences (2010), doi:10.1016/j.jseaes.2009.12.017

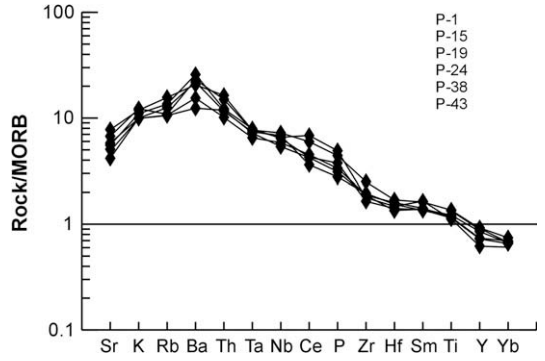

Fig. 5. MORB-normalized (Pearce, 1983) spidergrams for the representative samples from Polatlı volcanic rocks.

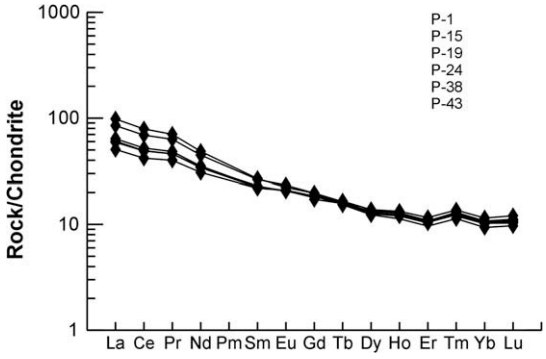

Fig. 6. Chondrite-normalized (Nakamura, 1974) REE patterns for the representative samples from Polatlı volcanic rocks.

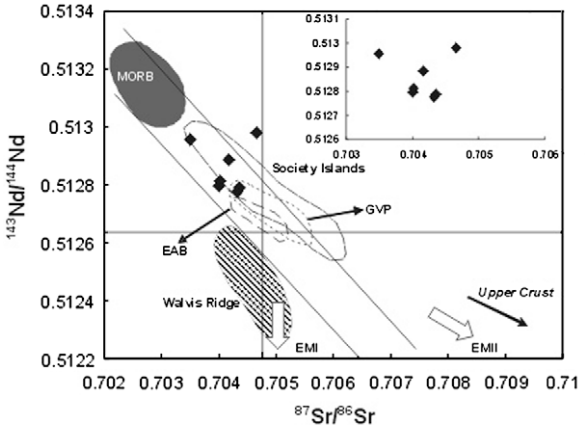

Fig. 7. $^{87}Sr/^{86}Sr$ vs.$^{143}Nd/^{144}Nd$ variation diagram of volcanic rocks of different tectonic environments compared to the Polatlı volcanic rocks. Data sources: Richardson et al. (1982), Ito et al. (1987), Dewey et al. (1990) and Varol Muratçay (2006). Mantle array and Bulk Earth from Wasserburg et al. (1981) and Faure (1986). EMI and EMII from Zindler and Hart (1986).

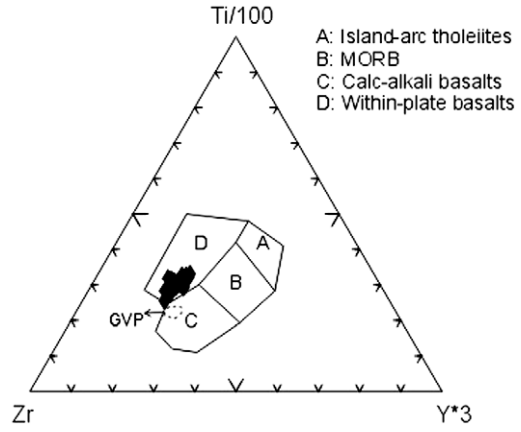

Fig. 8. Ti/100–Zr–Y*3 discrimination diagram of Pearce and Cann (1973) for the Polatlı volcanic rocks.

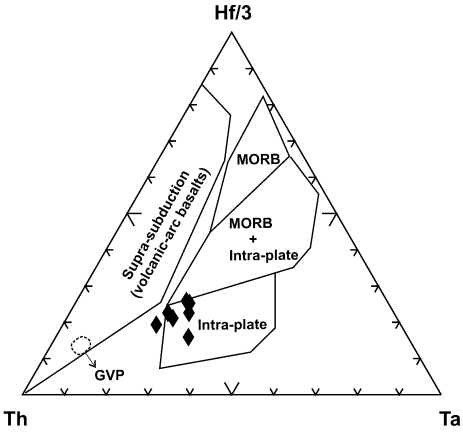

Fig. 9. Hf/3–Th–Ta tectonic discrimination diagram (Menzies et al., 1991) of Polatlı volcanic rocks.

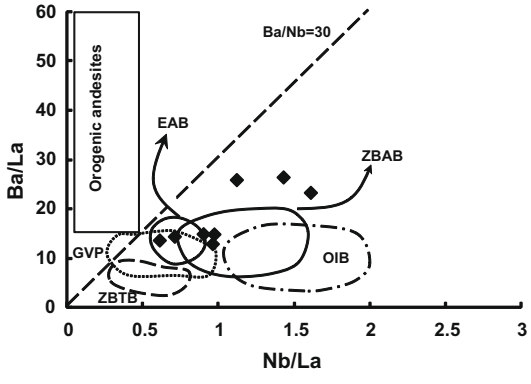

Fig. 10. Nb/La vs. Ba/La diagram of Polatlı volcanic rocks (data from McMillan and Dungan (1986), Altherr et al. (1988), Chaffey et al. (1989), Menzies et al. (1991), Class and Goldstein (1997), Widom et al. (1997), Kürkcüoğlu (2000) and Varol Muratçay (2006)).

active fracture with dip-slip to transtensional movements (Ocakoğlu, 2007). The older movements are of strike-slip character (Ocakoğlu, 2007). Neogene volcanic activities are reported along or near the Eskişehir fault zone (5.5 Ma, Servais, 1982; Miocene, Temel, 2001; 15.7 Ma, Ocakoğlu, 2007). We propose that the Polatlı activity is formed by fractures belonging to the Eskişehir fault zone.

Yağmurlu et al. (1988) studied the Miocene Beypazarı basin and concluded that the ca. 1000 m thick sedimentation is due to a N–S crustal extension. The study of a ENE-trending fault zone at the south of the GVP let Yürür et al. (2002) to propose that N–S crustal stretching produced the GVP magmatism in the Early Miocene. Finally, geochemical features of our data suggest that the Polatlı basaltic lavas formed in a intra-plate environment, during a rifting event marked by large-scale crustal events since the Early Miocene time.

Please cite this article in press as: Temel, A., et al. Alkaline series related to Early-Middle Miocene intra-continental rifting in a collision zone: An example from Polatlı, Central Anatolia, Turkey. Journal of Asian Earth Sciences (2010), doi:10.1016/j.jseaes.2009.12.017

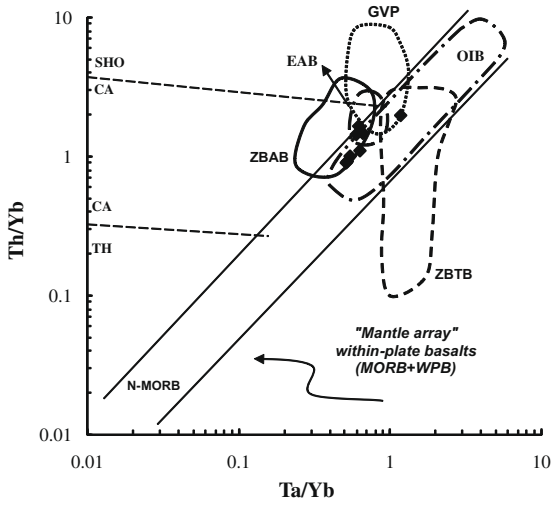

Fig. 11. Th/Yb vs. Ta/Yb diagram of Polatlı volcanic rocks (data from Chen and Frey (1985), Chen et al. (1990), McMillan and Dungan (1986), Ito et al. (1987), Altherr et al. (1988), Gerlach et al. (1988), Chaffey et al. (1989), Class and Goldstein (1997), Kürkcüoğlu (2000) and Varol Muratçay (2006)).

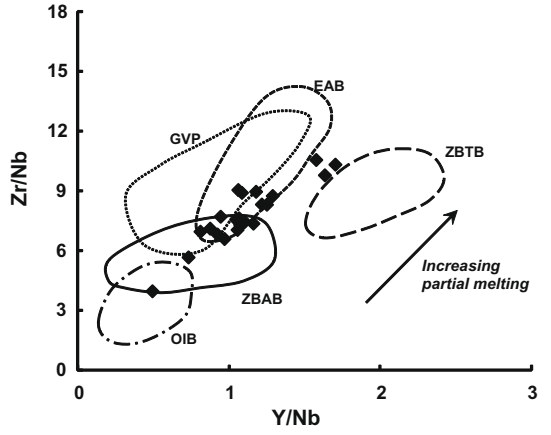

Fig. 12. Y/Nb vs. Zr/Nb diagram of Polatlı volcanic rocks (data from McMillan and Dungan (1986), Altherr et al. (1988), Chaffey et al. (1989), Menzies et al. (1991), Class and Goldstein (1997), Widom et al. (1997), Kürkcüoğlu (2000) and Varol Muratçay (2006)).

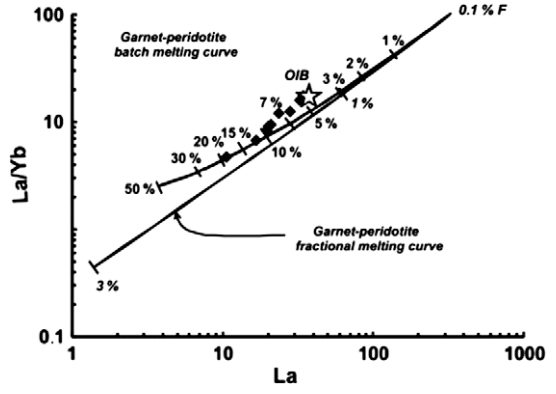

Fig. 13. La vs. La/Yb diagram of Polatlı volcanic rocks. Melt curves obtained from fractional and batch melting equations of Shaw (1970) are also shown.

There remains, however, a point that is not clear, the Early Miocene kinematics of the Eskişehir fault zone since we propose crustal extension and that the older movements of the fault zone are proposed to be of strike-slip character (Ocakoğlu, 2007). The Eskişehir fault trends ESE-WSW, similar to the present-day southern Aegean horst and grabens (e.g. Şengör and Kidd, 1979) whereas for a ENE-trending fault zone, about 100 km NE, Yürür et al. (2002) found field evidences to suggest that the fault accommodated ca. N–S extension during the Early Miocene in the GVP. Further field data is necessary to better constrain the chronology and nature of the different movements the Eskişehir fault seems to have accommodated.

8. Magma source differences between the GVP and Polatlı lavas

Geochemical data from the GVP and from the Polatlı volcanites (this study) attest clearly that these two coeval magmatic events being generated in places not far from each other (~100 km) are, however, associated with mantle sources with different compositions. The GVP magmatism is located on the Neo-Tethyan suture zone and generated by reactivation of this plate boundary in the post-collisional period. Its products show the characteristics of a mantle source modified by earlier subductional processes (Wilson et al., 1997; Varol Muratçay, 2006). In Polatlı, basaltic lavas erupted in the same time do clearly not display this characteristic and seem to be affected only by crustal contamination. We think that the mantle beneath the suture zone has preserved for about 20 My the chemical features of a mantle that was modified by the Late Cretaceous subduction (Görür et al., 1998). At about 100 km far from the suture zone, the subductional component disappears in the Polatlı magmatism. This distance of 100 km, not much modified by later crustal shortening, is therefore an upper limit estimate for the lateral extent of the subduction-modified part of the underlying mantle. It is also interesting to note that after a relatively short period of time (~8 My) of heavy magmatic activity in the GVP, the last magmatic production of Güvem basaltic rocks at about 10 My (Tankut et al., 1998) do also not bear the subductional signature of the underlying mantle in the GVP suggesting that this time interval that becomes about 12 My when considering the time elapsed since the end of the first significant activity (~14 My) and the last activity (Güvem) corresponds to the time where the mantle restores its "normal" composition after modifications due to the closure of an ocean. The production of huge volumes of magma in the Early Miocene may have considerably decreased this time interval.

9. Conclusions

We present field and geochemical data collected from the Polatlı flood basalts erupted during the Early and Middle Miocene times. In the same time, acid-intermediate magmatism was produced in the northern Galatean Volcanic Province (GVP). We show that Polatlı lavas originated from a mantle source different than that of the GVP volcanites, these regions being far from another by about 100 km. We attribute this difference in the source signature to the heterogeneity of the mantle, the crust of the northern GVP area being located on a mantle modified by the older Neo-Tethyan subduction whereas the Polatlı crust may be underlain by a mantle not chemically modified by this geotectonic event.

Products of a within-plate magmatism, the eruption of the Lower-Middle Miocene Polatlı basaltic rocks is contemporaneous with the formation of the Galatean Volcanic Province and the large Beypazarı basin. These geographically close events associated with N-S crustal extension substantiate the view that crustal rifting started to prevail in the early periods of the Neogene time in NW Central Anatolia.

Please cite this article in press as: Temel, A., et al. Alkaline series related to Early-Middle Miocene intra-continental rifting in a collision zone: An example from Polatlı, Central Anatolia, Turkey. Journal of Asian Earth Sciences (2010), doi:10.1016/j.jseaes.2009.12.017

Acknowledgements

This study is financed by a research project (number 99 01 602 007) of the Hacettepe University and the French Embassy in Ankara. The manuscript benefited from useful comments formulated by Georg Zellmer, an anonymous reviewer and the editor Bor-ming Jahn.

References

Akdağ, N., 2005. Mineralogical and geochemical investigation of neogene sedimentary units around Polatlı, Ankara, Turkey (in Turkish). M.Sc. Thesis, Hacettepe University, Institute of Pure Sciences, Ankara, p. 67 (unpublished).

Alıcı, P., Temel, A., Gourgaud, A., Kieffer, G., Gündoğdu, M.N., 1998. Petrology and geochemistry of potassic rocks in the Gölcük area (Isparta, SW Turkey): genesis of enriched alkaline magmas. Journal of Volcanology and Geothermal Research 85, 423–446.

Alıcı, P., Temel, A., Gourgaud, A., Vidal, P., Gündoğdu, M.N., 2001. Quaternary tholeiitic and alkaline volcanism in the Karasu Valley (Hatay, SE Turkey): Sr–Nd–Pb–O Isotopic compositions and trace element geochemistry. International Geology Review 43, 120–138.

Alıcı, P., Temel, A., Gourgaud, A., 2002. Pb–Nd–Sr isotope and trace element geochemistry of Quaternary extension-related alkaline volcanism: a case study of Kula region (western Anatolia, Turkey. Journal of Volcanology and Geothermal Research 115 (3–4), 487–510.

Altherr, R., Henjes-Kunst, F., Puchelt, H., Baumann, A., 1988. Volcanic activity in the Red Sea axial trough, evidence for a large mantle diapir. Tectonophysics 150, 121–133.

Bellon, H., Quoc Buu, N., Chaumont, J., Philippet, J.C., 1981. Implantation ionique d'argon dans une cible support: application au traçage isotopique de l'argon contenu dans les minéraux et les roches. Comptes Rendus de l'Académie des Sciences de Paris 292, 977–980.

Buket, E., Temel, A., 1998. Major-element, trace-element, and Sr–Nd isotopic geochemistry and genesis of Varto (Muş) volcanic rocks, Eastern Turkey. Journal of Volcanology and Geothermal Research 85 (1–4), 405–421.

Chaffey, D.J., Cliff, R.A., Wilson, B. M., 1989. Characterization of the St. Helena magma source. In: Saunders, A.D., Norry, M.J. (Eds.), Magmatism in the Ocean Basins, vol. 42, Geological Society Special Publication, pp. 257–276.

Chen, C.-Y., Frey, F.A., 1985. Trace element and isotopic geochemistry of lavas from Haleakala volcano, East Maui, Hawaii: implications for the origin of Hawaiian basalts. Journal of Geophysical Research 90, 8743–8768.

Chen, C.-Y., Frey, F.A., Garcia, M.O., 1990. Evolution of alkalic lavas at Haleakala volcano, East Maui, Hawaii. Major, trace element and isotopic constraints. Contribution of Mineralogy and Petrology 105, 197–218.

Class, C., Goldstein, S.L., 1997. Plume-lithosphere interaction in the ocean basins: constraints from the source mineralogy. Earth and Planetary Science Letters 150, 245–260.

Demirbağ, H., 2005. Tectonic evolution of the Çiledağ-Polatlı (Ankara) region (in Turkish). M.Sc. Thesis, Hacettepe University, Institute of Pure Sciences, Ankara, p. 62 (unpublished).

Dewey, C.W., Albarede, F., Cheminée, J.-L., Michard, A., Mühe, R., Stoffers, P., 1990. Active submarine volcanism on the Society Hotspot Swell (West Pacific): a geochemical study. Journal of Geophysical Research 95 (B4), 5049–5066.

Edwards, C., Menzies, M., Thirlwall, M., 1991. Evidence from Muriah, Indonesia, for the interplay of supra-subduction zone and intraplate processes in the genesis of potassic alkaline magmas. Journal of Petrology 32 (3), 555–592.

Erol, O., 1955. The correlation revision report belonging to 'Geological maps of W. Weingart 56/2, 56/4 (Sivrihisar) and 57/1, 57/3 (Ankara) sheets'. MTA Compilation Report, No. 2473.

Faure, G., 1986. Principles of Isotope Geology. John Wiley and Sons, Canada. p. 589.

Fitton, J.G., James, D., Kempton, P.D., Ormerod, D.S., Leeman, W.P., 1988. The role of lithospheric mantle in the generation of late Cenozoic basic magmas in the Western United States. Journal of Petrology (Special Issue), 331–349.

Frey, F.A., 1980. The origin of pyroxenites and garnet pyroxenites from salt lake crater, Oahu, Hawaii: trace element evidence. American Journal of Science 280, 427–449.

Fujimaki, H., Tatsumoto, M., Aoki, K., 1984. Partition coefficients of Hf, Zr, and REE between phenocrysts and groundmasses. Journal of Geophysical Research 89, 662–672.

Gautier, I., Weis, D., Mennessier, J.-P., Vidal, P., Giret, A., Loubet, M., 1990. Petrology and geochemistry of Kerguelen basalts (South Indian Ocean): evolution of the mantle sources from ridge to an intraplate position. Earth and Planetary Science Letters 100, 59–76.

Gerlach, D.C., Cliff, R.A., Davies, G.R., Norry, M.J., Hodgson, N., 1988. Magma sources of the Cape Verdes Archipelagos: isotopic and trace elements constraints. Geochimica et Cosmochimica Acta 48, 2469–2482.

Gill, J.B., 1981. Orogenic Andesites and Plate Tectonics. Springer-Verlag, New York. p. 138.

Görür, N., Tüysüz, O., Şengör, A.M.C., 1998. Tectonic evolution of the Central Anatolian Basins. International Geology Review 40, 831–850.

Güleç, N., 1991. Crust–mantle interaction in Western Turkey: implications from Sr and Nd isotope geochemistry of Tertiary and Quaternary volcanics. Geological Magazine 128 (5), 417–435.

Gülen, L., 1990. Isotopic characterization of Aegean magmatism and geodynamic evolution of the Aegean subduction. In: Savaşçın, M.Y., Eronat, A.H. (Eds.), IESCA-1990 Proceedings, vol. 2, pp. 143–166.

Hakyemez, Y., Barkut, M., Bilginer, E., Pehlivan, Ş., Can, B., Dager, Z., 1986. Geology of Ilgaz – Çankırı – Çadır and neighbourhood. MTA Compilation Report, No. 7298.

Inci, U., 1991. Miocene alluvial fan-alkali playa lignite–trona bearing deposits from an inverted basin in Anatolia: sedimentology and tectonic controls on deposition. Sedimentary Geology 71, 72–97.

Inci, U., Helvacı, C., Yağmurlu, F., 1988. Stratigraphy of Beypazarı Neogene Basin, Central Anatolia. Newsletters Stratigraphy 18 (3), 165–182.

Innocenti, F., Manetti, P., Mazzuoli, G., Pasquare, G., Villari, L., 1982. Anatolia and north-western Iran. In: Thorpe, R.S. (Ed.), Orogenic Andesites and Related Rocks. J.Wiley and Sons, New York, pp. 327–349.

Ionov, D., Harmer, R.E., 2002. Trace element distribution on calcite–dolomite carbonatites from Spitskop: inferences for differentiation of carbonatite magmas and the origin of carbonates in mantle xenoliths. Earth and Planetary Science Letters 198, 495–510.

Ionov, D.A., Savoyant, L., Dupuy, C., 1992. Application of the ICP-MS to trace element analysis of peridotites and their minerals. Geostandards Newletter 16, 311–315.

Irving, A.J., Frey, F.A., 1978. Distribution of trace elements between garnet megacrysts and host volcanic liquids of kimberlitic to rhyolitic composition. Geochimica Cosmochima Acta 42, 771–787.

Ito, E., White, W.M., Göpel, C., 1987. The O, Sr, Nd and Pb isotope geochemistry. Chemical Geology 62, 157–176.

Jung, S., Masberg, P., 1998. Major and trace element systematics and isotope geochemistry of Cenozoic mafic volcanic rocks from the Vogelsberg (Central Germany): constraints on the origin of continental alkaline and tholeiitic basalts and their mantle sources. Journal of Volcanology and Geothermal Research 86, 151–177.

Keller, J., Jung, D., Eckhardt, F.J., Kreuzer, H., 1992. Radiometric ages and chemical characterization of the Galatean andesite massif, Pontus, Turkey. Acta Vulcanologica Marinelli 2, 267–276.

Koçyiğit, A., Türkmenoğlu, A., Beyhan, A., Kaymakçı, N., Akyol, E., 1995. Post-collisional tectonics of Eskisehir – Ankara –Çankırı Segment of Izmir – Ankara – Erzincan Suture Zone: Ankara Orogenic Phase. Turkish Association of Petroleum Geologists Bulletin 6 (1), 69–86.

Koçyiğit, A., Winchester, J.A., Bozkurt, E., Holland, G., 2003. Saraçköy Volcanic Suite: implications for the subductional phase of arc evolution in the Galatean Arc Complex, Ankara, Turkey. Geological Journal 38 (1), 1–14.

Kürkcüoğlu, B., 2000. The geochemical evolution of the Erciyes stratovolcano (in Turkish). PhD Thesis, Hacettepe University, Institute of Pure Sciences, Ankara, p. 145 (unpublished).

Kürkcüoğlu, B., Sen, E., Aydar, E., Gourgaud, A., Gündoğdu, M.N., 1998. Geochemical approach to magmatic evolution of Mt. Erciyes stratovolcano, Central Anatolia, Turkey. Journal of Volcanology and Geothermal Research 85 (1–4), 473–494.

Le Bas, M.J., Le Maitre, R.W., Streckeisen, A., Zanetti, B., 1986. A chemical classification of volcanic rock based on the total alkali – silica diagram. Journal of Petrology 27, 745–750.

Mahood, G., Drake, R.E., 1982. K–Ar dating young rhyolite rocks: a case study of the Sierra La Primavera, Jalisco, Mexico. Geological Society of America Bulletin 93, 1232–1241.

McMillan, N.J., Dungan, M.A., 1986. Magma mixing as a petrogenetic process in the development of the Taos plateau volcanic fields, New Mexico. Journal of Geophysical Research 91 (B6), 6029–6045.

Menzies, M.A., Kyle, P.R., Jones, M., Ingram, G., 1991. Enriched and depleted source components for tholeiitic and alkaline lavas from Zuni-Bandera New Mexico: inferences about intraplate processes and stratified lithosphere. Journal of Geophysical Research 96, 13645–13671.

Miyashiro, A., 1978. Nature of alkalic volcanic rock series. Contribution of Mineralogy and Petrology 66, 91–104.

Morimoto, N., 1988. Nomenclature of pyroxenes. Bulletin of Mineralogy 111, 535–550.

Nakamura, N., 1974. Determination of REE, Ba, Fe, Mg, Na and K in carbonaceous and ordinary chondrites. Geochimica Cosmochimica Acta 38, 757–775.

Notsu, K., Fujitani, T., Ui, T., Matsuda, J., Ercan, T., 1995. Geochemical features of collision-related volcanic rocks in central and eastern Anatolia, Turkey. Journal of Volcanology and Geothermal Research 64, 171–192.

Ocakoğlu, F., 2007. A re-evaluation of the Eskisehir Fault Zone as a recent extensional structure in NW Turkey. Journal of Asian Earth Science 31, 91–103.

Pearce, J.A., 1983. Role of subcontinental lithosphere in magma genesis at active continental margins. In: Hawkesworth, C.J., Norry, M.J. (Eds.), Continental Basalts and Mantle Xenoliths. Shiva Publishing Limited, Nantwich, Cheshire, pp. 230–249.

Pearce, J.A., Cann, J.R., 1973. Tectonic setting of basic volcanic rocks determined using trace element analysis. Earth and Planetary Science Letters 19, 290–300.

Pearce, J.A., Bender, J.F., De Long, S.E., Kidd, W.S.F., Low, P.J., Güner, Y., Şaroğlu, F., Yılmaz, Y., Moorbath, S., Mitchell, J.G., 1990. Genesis of collision volcanism in Eastern Anatolia, Turkey. Journal of Volcanology and Geothermal Research 44, 189–229.

Richardson, S.H., Erlank, A.J., Duncan, A.R., Reid, D.L., 1982. Correlated Nd, Sr and Pb isotope variation in Walvis Ridge basalts and implications for the evolution of their mantle source. Earth and Planetary Science Letters 59, 327–342.

Rollinson, H.R., 1993. Using geochemical data: evaluation, presentation, interpretation, Longman Scientific and Technical. John Wiley and Sons Inc., New York. p. 352.

Please cite this article in press as: Temel, A., et al. Alkaline series related to Early-Middle Miocene intra-continental rifting in a collision zone: An example from Polatlı, Central Anatolia, Turkey. Journal of Asian Earth Sciences (2010), doi:10.1016/j.jseaes.2009.12.017

Saunders, A.D., Norry, M.J., Tarney, J., 1988. Origin of MORB and chemically-depleted mantle reservoirs: trace element constraints. Journal of Petrology (Special Lithosphere Issue), 415–445.

Savascın, M. Y., 1990. Magmatic activities of Cenozoic compressional and extensional tectonic regimes in Western Anatolia. IESCA, 1990, Turkey, Proceedings, pp. 421–434.

Savascın, M.Y., Güleç, N., 1990. Relationship between magmatic and tectonic activities in Western Turkey. IESCA 1990, Turkey 2, 300–314.

Şengör, A. M. C., 1980. Türkiye'nin Neotektoniğinin Esasları (Essentials of the Turkish Neotectonics) in Turkish. In: Ankara, T.J.K. (Ed.), Conference series, vol. 2, p. 40.

Şengör, A.M.C., Kidd, W.S.F., 1979. Post-collisional tectonics of the Turkish–Iranian plateau and a comparison with Tibet. Tectonophysics 55, 361–376.

Şengör, A.M.C., Görür, N., Şaroğlu, F., 1985. Strike-slip faulting and related basin formation in zone of tectonic escape: Turkey as a case study. In: Biddle, T.R., Christie-Blick, N. (Eds.), Strike-slip Deformation, Basin Formation and Sedimentation, Society of Economic Paleontologists and Mineralogists Special Publication, vol. 37, pp. 227–264.

Servais, M., 1982. Collision et suture Tethysienne en Anatolie Centrale:Etude structuralle et metamorphique (HP-BT) de la zone Nord Kütahya. Ph. D. Thesis, L'universite de Paris-Sud, Centre D'Orsay, 374pp (unpublished).

Seyitoğlu, G., Büyükönal, G., 1995. Geochemistry of Ankara volcanics and the implications of their K–Ar dates on the Cenozoic stratigraphy of central Turkey. Turkish Journal of Earth Sciences 4, 87–92.

Shaw, D.M., 1970. Trace element fractionation during anatexis. Geochimica Cosmochimica Acta 34, 237–243.

Siyako, M., 1984. Temperature and geothermal gradients of the Thrace Basin. TPAO Unpublished Company Report, p. 30.

Steiger, R.H., Jäger, E., 1977. Subcommission on geochronology: convention on the use of decay constants in geo and cosmochronology. Earth Planetary Science Letters 36 (3), 359–362.

Tankut, A., Wilson, M., Yihunie, T., 1998. Geochemistry and tectonic setting of Tertiary volcanism in the Güvem area, Anatolia, Turkey. Journal of Volcanology and Geothermal Research 85, 285–301.

Temel, A., 2001. Post-Collisional Miocene alkaline volcanism in the Oğlakçı region, Turkey: petrology and geochemistry. International Geology Review 43, 640–660.

Temel, A., Gündoğdu, M.N., Gourgaud, A., 1998a. Petrological and geochemical characteristics of Cenozoic high-K calc-alkaline volcanism in Konya, central Anatolia, Turkey. Journal of Volcanology and Geothermal Research 85 (1–4), 327–354.

Temel, A., Gündoğdu, M.N., Gourgaud, A., Le Pennec, J.L., 1998b. Ignimbrites of Cappadocia (Central Anatolia, Turkey): petrology and geochemistry. Journal of Volcanology and Geothermal Research 85 (1–4), 447–471.

Temel, A., Gourgaud, A., Alıcı, P., Bellon, H., 2000. The role of asthenospheric mantle in the generation of Tertiary basaltic alkaline volcanism in the Polatlı – Ankara region, central Anatolia, Turkey: constraints from major-element, trace-element and Sr–Nd isotopes, Goldschmidt 2000, September 3–8th, 2000. Journal of Conference abstracts 5 (2), 989.

Thompson, R.N., 1982. Magmatism of the British Tertiary province. Scottish Journal Geology 18, 49–107.

Thompson, R.N., Morrison, M.A., Dickin, A.P., Hendry, G.L., 1983. Continental flood basalts. Arachnids rule OK? In: Hawkesworth, C.J., Norry, M.J. (Eds.), Continental Basalts and Mantle Xenoliths, pp. 158–185.

Tokel, S., 1984. Mechanism of crustal deformation in eastern Anatolia and the petrogenesis of young volcanites: In: Ketin Symposium Proceedings, pp. 121–130 (in Turkish with English abstract).

Tokel, S., Ercan, T., Akbaşlı, A., Yıldırım, T., Fişekçi, A., Selvi, Y., Ölmez, M., Can, B., 1988. Neogene tholeiitic province of Central Anatolia: implications for magma genesis and post-collision lithospheric dynamics. METU, Journal of Pure and Applied Sciences, Ankara 21, 461–477.

Toprak, V., Türkecan, A., 1998. Geology of the Galatean Volcanic Province, Turkey. In: Third International Turkish Geology Symposium, Excursion Guidebook.

Ünalan, G., Yüksel, V., Tekeli, T., Gönenç, O., Seyirt, Z., Hüseyin, S., 1976. The stratigraphy and palaeogeographical evolution of the upper Cretaceous-lower Tertiary sediments in the Haymana – Polatlı region (SW of Ankara). Bulletin of the Geological Society of Turkey 19 (2), 159–176.

Varol, E., Temel, A., Gourgaud, A., Bellon, H., 2007. Early Miocene 'adakite-like' volcanism in the Balkuyumcu region, central Anatolia, Turkey: petrology and geochemistry. Journal of Asian Earth Sciences 30, 613–628.

Varol, E., Temel, A., Gourgaud, A., 2008. Textural and compositional evidences for magma mixing in the evolution of Çamlıdere volcanic rocks (Galatean Volcanic Province), Central Anatolia, Turkey. Turkish Journal of Earth Sciences 17, 709–727.

Varol Muratçay, E., 2006. The petrology and geochemistry of the volcanic rocks from Camlıdere district (NW Ankara) (in Turkish). PhD Thesis, Hacettepe University, Institute of Pure Sciences, Ankara, p. 152 (unpublished).

Wasserburg, G.J., Jacobsen, S.B., DePaolo, D.J., McCulloch, M.T., Wen, T., 1981. Precise determination of Sm/Nd ratios, samarium, and neodymium isotopic abundances in standard solutions. Geochimica Cosmochimica Acta 45, 2311–2323.

Widom, E., Carlson, R.W., Gill, J.B., Schmincke, H.U., 1997. Th–Sr–Nd–Pb isotope and trace element evidence for the origin of the Sao Miguel, Azores, enriched mantle source. Chemical Geology 140, 49–68.

Wilson, M., 1989. Igneous Petrogenesis. Unwin Hyman Ltd., London, UK. p. 466.

Wilson, M., Tankut, A., Güleç, N., 1997. Tertiary volcanism of the Galatia province, north-west Central Anatolia, Turkey. Lithos 42, 105–121.

Yağmurlu, F., Helvacı, C., Inci, U., Önal, M., 1988. Tectonic characteristics and structural evolution of the Beypazarı and Nallıhan Neogene Basins, Central Anatolia. METU Journal of Pure and Applied Sciences, Ankara 21 (1–3), 127–143.

Yılmaz, Y., 1990. Comparison of young volcanic associations of western and eastern Anatolia formed under a compressional regime: a review. Journal of Volcanology and Geothermal Research 44, 69–87.

Yurtyeri, E., 1989. Geology, petrology and geochemistry of the Kanarakaya basalts, Polatlı, Ankara (in Turkish), MSc Thesis, METU, Department of geological Engineering, Ankara, Turkey, p. 67 (unpublished).

Yürür, M.T., Temel, A., Köse, O., 2002. Evidences of extensional tectonics at the southern boundary of the Galatean Volcanic Province, NW Central Anatolia. Bulletin of the Turkish Geological Society 45 (1), 85–98.

Zindler, A., Hart, S., 1986. Chemical geodynamics. Annual Review of Earth and Planetary Sciences 14, 493–571.

Please cite this article in press as: Temel, A., et al. Alkaline series related to Early-Middle Miocene intra-continental rifting in a collision zone: An example from Polatlı, Central Anatolia, Turkey. Journal of Asian Earth Sciences (2010), doi:10.1016/j.jseaes.2009.12.017